SYS-1/beta-catenin inheritance and regulation by Wnt-signaling during asymmetric cell division.

Maria F. Valdes Michel[1] and Bryan T. Phillips[1,2*]

[1] Interdisciplinary Graduate Program in Genetics, University of Iowa, Iowa City, IA.

[2] Department of Biology, University of Iowa, Iowa City IA.

***Corresponding author**
Email: bryan-phillips@uiowa.edu

Key words: Wnt, SYS-1, beta-catenin, asymmetric cell division, *C. elegans,* APC

Abstract

Asymmetric cell division (ACD) allows daughter cells of a polarized mother to acquire different developmental fates. In *C. elegans*, the Wnt/β-catenin Asymmetry (WβA) pathway oversees many embryonic and larval ACDs; here, a Wnt gradient induces an asymmetric distribution of Wnt signaling components within the dividing mother cell. One terminal nuclear effector of the WβA pathway is the transcriptional activator SYS-1/β-catenin. SYS-1 is sequentially negatively regulated during ACD; first by centrosomal regulation and subsequent proteasomal degradation and second by asymmetric activity of the β-catenin "destruction complex" in one of the two daughter cells, which decreases SYS-1 levels in the absence of WβA signaling. However, the extent to which mother cell SYS-1 influences cell fate decisions of the daughters is unknown. Here, we quantify inherited SYS-1 in the differentiating daughter cells and the role of SYS-1 inheritance in Wnt-directed ACD. Photobleaching experiments demonstrate the GFP::SYS-1 present in daughter cell nuclei is comprised of inherited and *de novo* translated SYS-1 pools. We used a photoconvertible DENDRA2::SYS-1, to directly observe the dynamics of inherited SYS-1. Photoconversion during mitosis reveals that SYS-1 clearance at the centrosome preferentially degrades older SYS-1, and this accumulation is regulated via dynein trafficking. Photoconversion of the EMS cell during Wnt-driven ACD shows daughter cell inheritance of mother cell SYS-1. Additionally, loss of centrosomal SYS-1 increased inherited SYS-1 and, surprisingly, loss of centrosomal SYS-1 also resulted in increased levels of *de novo* SYS-1 in both EMS daughter cells. Lastly, we show that daughter cell negative regulation of SYS-1 via the destruction complex member APR-1/APC is key to limit both the *de novo* and the inherited SYS-1 pools in both the E and the MS cells. We conclude that regulation of both inherited and newly translated SYS-1 via centrosomal processing in the mother cell and daughter cell regulation via Wnt signaling are critical to maintain sister SYS-1 asymmetry during ACD.

Introduction

Asymmetric cell division (ACD) is an essential mechanism that controls cell fate specification during development and adult tissue homeostasis. ACD increases the developmental cell diversity needed for functional tissues, including such diverse and well-studied examples as *C. elegans* embryos, *Drosophila* neuroblasts, and mammalian lung epithelial cells (NEUMÜLLER AND KNOBLICH 2009; CHHABRA AND BOOTH 2021; KOCHENDOERFER *et al.* 2021). During adulthood, ACD maintains tissue integrity by promoting stem cell self-renewal while also producing cells that will further differentiate to repopulate dying or degraded tissues (YAMASHITA *et al.* 2010). Given that ACDs of stem cells maintain the ability to replenish damaged or growing tissues even post-development, tight regulation of these stem cell niches is needed to prevent tumorigenesis. Accordingly, when pathways that regulate ACD go awry, the risk of cancer increases (MORRISON AND KIMBLE 2006). Both tumorigenesis and development use self-renewal and proliferation to drive progression, which often occurs via regulation of the same signaling pathways. Thus, understanding the mechanism regulating ACDs will contribute to the understanding of how cell fate specification occurs during development and will illuminate the mechanism by which tumors develop (BAJAJ *et al.* 2015).

The Wnt/β-catenin pathway is a well-conserved signaling pathways that regulate stem cell maintenance, cell renewal and differentiation, cell polarity, and ACD (RING *et al.* 2014; CHEN *et al.* 2022; HABIB AND ACEBRÓN 2022; HAYAT *et al.* 2022). In this pathway, Wnt ligands activate a signal transduction cascade that stabilizes the coactivator β-catenin. Stabilized β-catenin translocates into the nucleus which initiates transcription of Wnt target genes. In the absence of Wnt ligand, β-catenin is degraded by a "destruction complex" which is comprised of casein kinase 1α (CK1α), glycogen synthase kinase 3β (GSK3β), and two scaffolds, Axin and adenomatous polyposis coli (APC). Without β-catenin in the nucleus, the transcription factor T-cell factor (TCF) acts as a transcriptional repressor of Wnt-target genes (LIN *et al.* 1998; MACDONALD *et al.* 2009). Because the Wnt/β-catenin signaling pathway plays a critical role in cell polarity, ACD, development, and organismal homeostasis, mutations and misregulation of this pathway lead to cell fate dysregulation. Aberrant regulation of Wnt signaling is a common theme of cancer biology. Hyperactivation of Wnt signaling often leads to malignant transformation (DE LA ROCHE *et*

al. 2008; POLAKIS 2012). Tumor sequencing further reveals frequent inactivating mutations in APC and activating mutations in β-catenin(GILES *et al.* 2003; OBRADOR-HEVIA *et al.* 2010; QU *et al.* 2016). Constitutive Wnt pathway activity is present in 90% of colorectal cancer cases. This may be impacted by changes in the cell polarity and in ACD, which leads to an increase in the cellular proliferation of the epithelial stem cell population of the intestine (GILES *et al.* 2003; QUYN *et al.* 2010). Even though regulation of β-catenin is essential for proper Wnt signaling, how the mother cell distributes β-catenin into the daughter cells and how β-catenin is differentially regulated during ACD remains unclear.

C. elegans is an excellent model organism to uncover the mechanisms by which the Wnt/β-catenin signaling pathway regulates ACDs. The Wnt/β-catenin asymmetry (WβA) pathway oversees many embryonic and larval ACDs through regulation of the *C. elegans* β-catenin, SYS-1 (KIDD *et al.* 2005; HUANG *et al.* 2007; PHILLIPS AND KIMBLE 2009). The WβA pathway is a branched pathway specialized for ACD that uses a β-catenin paralog, WRM-1 and SYS-1, in each branch (ROCHELEAU *et al.* 1999; LO *et al.* 2004; KIDD *et al.* 2005; PHILLIPS *et al.* 2007; SUGIOKA *et al.* 2011; ROBERTSON AND LIN 2012). One branch activates the nuclear export of approximately 50% of the TCF/LEF DNA-binding protein, POP-1, via association with WRM-1 (LO *et al.* 2004). WRM-1-assisted export of POP-1 is, counterintuitively, required for Wnt-target gene activation likely because POP-1 functions as a transcriptional repressor when not bound to β-catenin/SYS-1 (ROCHELEAU *et al.* 1999; LO *et al.* 2004). POP-1 nuclear export enables the remaining nuclear POP-1 to form a complex with its coactivator β-catenin/SYS-1 (KIDD *et al.* 2005; YANG *et al.* 2015). The second branch of the WβA pathway regulates the stabilization and subsequent nuclear localization of SYS-1, in which SYS-1 ultimately controls transcription of Wnt-target genes by complexing with POP-1 (MIZUMOTO AND SAWA 2007; BALDWIN AND PHILLIPS 2014).

SYS-1 is broadly expressed at the transcriptional level but expression, including asymmetric expression, is tightly regulated at the protein level (HUANG *et al.* 2007; PHILLIPS *et al.* 2007). One example of regulation of SYS-1 protein expression is via centrosomal localization and subsequent turnover. SYS-1 symmetrically localizes to the centrosomes during ACD, and that SYS-1 centrosomal localization is dependent on the centrosomal protein, regulator of spindle assembly 2 (RSA-2) (HUANG *et*

al. 2007; PHILLIPS *et al.* 2007; SCHLAITZ *et al.* 2007; CHRISTIAN 2012; VORA AND PHILLIPS 2015; VORA AND PHILLIPS 2016). RSA-2 depletion demonstrates that RSA-2 is required for SYS-1 centrosomal localization in embryonic mother cells (VORA AND PHILLIPS 2015; VORA AND PHILLIPS 2016). After ACD, overall SYS-1 protein levels, including nuclear SYS-1, increase in both daughter cells in the absence of RSA-2. The increase of overall SYS-1 after RSA-2 depletion suggests centrosomal regulation leads to the negative regulation and subsequent degradation of centrosomally localized SYS-1. Thus, negative regulation of SYS-1 via centrosomal localization normally limits the levels of SYS-1 in the daughter cells resulting from an ACD. Depletion of the proteasome core ATPase subunit of the 26S proteasome, RPT-4, results in elevated and stabilized centrosomal SYS-1 and decreased SYS-1 turnover compared to wild type (VORA AND PHILLIPS 2015; VORA AND PHILLIPS 2016). These results are consistent with the hypothesis that the centrosomal proteasome plays a key role in regulating SYS-1 turnover at the centrosome via active degradation by the proteasome.

The microtubule motor dynein enhances the rapid accumulation of SYS-1 on mitotic centrosomes of large embryonic blastomeres via microtubule trafficking of SYS-1 (THOMPSON *et al.* 2022), leading to SYS-1 mitotic turnover. Thus, dynein works as a negative regulator of ACD, by enhancing centrosomal SYS-1 levels and subsequent SYS-1 degradation by the centrosomal proteasome. Knockdown of single dynein subunits, including heavy chain DHC-1 or the light chain subunits DLC-1 and DYLT-1, lead to reduced SYS-1 centrosomal enrichment and elevated SYS-1 in both daughter cells. Additionally, loss of these dynein complex subunits results in the conversion of larval ACDs to symmetric divisions, increasing the Wnt-signaled cell fates (THOMPSON *et al.* 2022). These data highlight the importance of microtubule trafficking for SYS-1 centrosomal localization and subsequent degradation. However, when treating embryos with the drug nocodazole to disable microtubule polymerization and subsequent microtubule trafficking, a surprising increase of cytoplasmic and centrosomal SYS-1 was observed, in addition to a less mobile SYS-1 compared to wild type (THOMPSON *et al.* 2022). These data, therefore, suggest that a negative regulator of SYS-1 is also trafficked to the centrosome by the dynein motor that regulates SYS-1 levels. The nocodazole phenotype is similar to that of RPT-4 depletion, which also resulted in elevated centrosomal SYS-1 (VORA AND PHILLIPS 2015; VORA AND PHILLIPS 2016), indicating

that the trafficked negative regulator may be the proteasome itself. Strengthening this hypothesis, when the worm homolog of mammalian proteasomal trafficking factor ECM29 (LEGGETT *et al.* 2002), *ecps-1,* is depleted, embryos with increased centrosomal SYS-1 were observed, in addition to a second substrate of the centrosomal proteasome, ZYG-1 (PEEL *et al.* 2012; THOMPSON *et al.* 2022). Thus, the current model suggests that SYS-1 and the proteasome are both actively trafficked via dynein to the centrosome during mitosis and, upon proper localization, result in SYS-1 degradation. This model reconciles the observed increase in centrosomal SYS-1 after nocodazole treatment because SYS-1 is more likely to be passively trafficked to the centrosome via diffusion compared to the large proteasome complex. The observed increase in cytoplasmic SYS-1 following RPT-4 knockdown further supports the model in which loss of SYS-1 negative regulation affects its degradation and turnover (THOMPSON *et al.* 2022).

While the above model details SYS-1 negative regulation via centrosomal localization during mitosis in the mother cell, SYS-1 is also regulated after an ACD by the β-catenin destruction complex under the regulatory control of WβA in the daughter cells. In response to the Wnt ligand gradient, the WβA pathway polarizes the mother cell and distributes different components of the Wnt-signaling pathway to anterior or posterior poles before mitosis. The positive Wnt regulators, Frizzled and Disheveled, are asymmetrically localized at the posterior cortex, resulting in their enrichment in Wnt-signaled daughter cell after cytokinesis (PARK *et al.* 2004; HARRELL AND GOLDSTEIN 2011; SAWA AND KORSWAGEN 2013; LAM AND PHILLIPS 2017). Negative regulators and members of the destruction complex, APC and Axin, are localized at the anterior pole of the mother cell and are asymmetrically enriched in the anterior Wnt-unsignaled daughter cell. The worm homolog of APC, APR-1, is essential for SYS-1 negative regulation during ACD (ROCHELEAU *et al.* 1997; BARTH *et al.* 2008; BALDWIN AND PHILLIPS 2014). The polar cortical localization of APR-1 is controlled by the worm Axin homolog, PRY-1, which regulates the asymmetry of SYS-1. These data, coupled with the above centrosomal regulation data, suggest the current model of SYS-1 regulation occurs via centrosomal degradation of mother cell SYS-1 and asymmetric regulation of *de novo* synthesized SYS-1 by the destruction complex in the Wnt-signaled and -unsignaled daughter cells (MIZUMOTO AND SAWA 2007; BALDWIN AND PHILLIPS 2014).

The current model suggests that centrosomal degradation of mother cell SYS-1 may be complete

to prevent inheritance into the daughter cells to ensure proper asymmetric SYS-1 regulation. However, lineage studies show that the Wnt-signaled daughters of Wnt-signaled cells respond more strongly to Wnt signaling in the subsequent division compared to their cousins, the Wnt-signaled daughters of Wnt-unsignaled cells (ZACHARIAS *et al.* 2015; ZACHARIAS AND MURRAY 2016). The heightened response can be visualized by both an enrichment of SYS-1 in the nucleus and increased target gene transcription (ZACHARIAS *et al.* 2015; ZACHARIAS AND MURRAY 2016). This nuclear SYS-1 enrichment suggests SYS-1 may be shielded from proteasomal degradation during nuclear localization, allowing for SYS-1 inheritance into the daughter cells of previously Wnt-signaled mother cells and progressively enriching the Wnt-signaled lineages for SYS-1 over time. Alternatively, enrichment of positive regulators of SYS-1 in Wnt-signaled lineages, such as Frizzled or Dishevelled (SAWA *et al.* 1996; UMBHAUER *et al.* 2000), would also be predicted to increase downstream SYS-1 stabilization. In this latter case, inheritance of upstream Wnt pathway components would be expected to similarly increase WRM-1 and decrease nuclear POP-1 levels between cousins, which was indeed observed in this study (LIN *et al.* 1998; ZACHARIAS *et al.* 2015; ZACHARIAS AND MURRAY 2016). This suggests that increased SYS-1 inheritance from signaled mothers is unlikely to be the sole mechanism of cousin enrichment. However, the extent to which direct SYS-1 inheritance contributes to a Wnt pathway “memory” during normal ACD and how Wnt signaling regulates inherited and *de novo* SYS-1 remains unknown.

Here, we show centrosomal degradation of SYS-1 in the EMS mother cell is incomplete, leading to SYS-1 inheritance in the E and the MS daughter cells during wild-type ACDs. We developed a photoconvertible SYS-1 to observe the dynamics of preexisting and newly synthesized SYS-1 at the centrosome during mitosis. We found that preexisting and newly synthesized SYS-1 levels are trafficked to the mitotic centrosome via the dynein complex where they are both degraded. SYS-1 coupling, trafficking, and degradation at the mother cell centrosome are necessary for maintaining sister cell asymmetry and wild-type SYS-1 asymmetry in E and MS daughter cells during ACD. Surprisingly, *de novo* SYS-1 increases in both daughter cells after the over-inheritance of mother cell SYS-1 during asymmetric cell division. Additionally, depletion of the negative regulator APR-1 increased both pools of SYS-1 in the E and MS nuclei, suggesting that, when inherited SYS-1 is affected, *de novo* SYS-1 is also

misregulated and vice versa. Thus, we propose a model in which SYS-1 centrosomal degradation is a key regulator of SYS-1 inheritance that prevents the loss of daughter cell asymmetry. Further regulation of inherited and *de novo* SYS-1 in the E and MS daughter cells via Wnt signaling supports proper sister cell asymmetry due to a free exchange between the inherited and *de novo* SYS-1 pools.

Methods

Strains

Strains were maintained on OP50-inoculated nematode growth media (NGM) plates at 20°C (PHX5708 and N2) or 25°C (TX964) using typical *C. elegans* methods (BRENNER 1974). The genotypes of the investigated are as follows: N2 (wild type); TX964 (unc-119(ed3) III; him-3(e1147) IV; teIs98 [P_{pie-1}::GFP::SYS-1]); BTP254 *(syb5708[*$P_{sys-1::}$DENDRA2::SYS-1*])*.

CRISPR/Cas9 mediated fluorescent tagging of endogenous SYS-1

An in-frame N-terminal DENDRA2-GAS tag was inserted in the endogenous *sys-1* gene prior to the endogenous start codon (SunyBioTech, Fujian, China). Two synonymous nucleotide changes were generated in the donor sequence to prevent the donor from being recognized and cut by Cas9. Genome edited animals were sequence verified with DENDRA-2-*sys-1* specific primers and backcrossed to wild-type N2 worms to reduce the chances of extraneous genetic variation or off target insertions impacting our experiments. The resulting strain, *sys-1(syb5708[*$P_{sys-1::}$DENDRA2::SYS-1*]),* is designated by strain name BTP254.

RNAi

To perform RNAi knockdown of target genes, we used HT115 bacteria containing the pL4440 plasmid with a T7-flanked target gene insert. *rsa-2*, *apr-1* and *ecps-1* were obtained from a library supplied by Ahringer (Addgene) (KAMATH *et al.* 2003). *dlc-1* was obtained from the Phillips lab library and made as described in Thompson *et* al., 2022. Briefly, *dlc-1* was amplified using target gene-flanking primers and *C. elegans* cDNA to generate a new insert. Bacteria with the desired insert were seeded onto

isopropyl β-d-1-thiogalactopyranoside (IPTG)-containing plates to induce transcription from the T7 promotor as described previously (CONTE *et al.* 2015). Worms were plated onto RNAi bacterial lawns after sodium hypochlorite synchronization as L1s, with the exception of worms plated on *dlc-1* bacterial lawns which were washed from OP50 plates at 24 h before imaging (L3/L4) and plated on to the RNAi plate to avoid larval phenotypes (TIMMONS 2006; BEKAS AND PHILLIPS 2020).

Confocal microscopy and FRAP

Confocal microscopy was performed with a Leica SP8 HyD detector system. The objective used was a 63× HC PL APO CS2 objective with N.A. = 1.4, using type F immersion oil. Each analyzed image consisted of 35 summed z-images of the embryo, with each slice approximately 0.6-µm thick. FRAP was performed on the same system. Each embryo was imaged once then photobleached, at anaphase, telophase or cytokinesis. The entire EMS cell was selected as the region of interest (ROI) and bleached at an intermediate focal plane with 100% laser power for 200 iterations. Images were taken immediately after photobleaching at 4, 6, 8 and 10 minutes. Fluorescence intensity was measured on the sum of 6 Z-projection slices in FIJI using the mean fluorescence intensity of ROIs around the nuclei of the E and MS cells.

Confocal microscopy and photoconversion of DENDRA2::SYS-1

Confocal microscopy was performed via a Leica SP8 HyD detector system using a 63× HC PL APO CS2 objective with N.A. = 1.4 and type F immersion oil. Each image analyzed consisted of the sum of 35 z-images, approximately 0.6-µm thick, across the embryo. Photoconversion of DENDRA2::SYS-1 was performed on the same system. For centrosome and cytoplasm photoconversion the FRAP software was used to photoconvert the desired locale. Before photoconversion, one image was taken in early metaphase to observe and quantify pre-conversion green SYS-1 levels at the centrosome. The ROI was then photoconverted using the UV laser (405nm diode laser) at an intermediate focal plane with 100% laser power for 200 iterations. Excitation light at 488 nm (490–550 nm) or 552 nm (580–670 nm) was provided by HyD lasers set at 30% laser power for both channels on standard mode. Images were taken

immediately after photoconversion every 20 seconds through mitosis of the P1 cell with a frame and line average of 2. To obtain the CEI, the mean intensity of the embryonic cytoplasm was subtracted from the centrosomal mean (THOMPSON *et al.* 2022).

For whole embryo photoconversion and quantification of DENDRA2::SYS-1 nuclear levels in the E and MS daughter cells, embryos were exposed to a UV laser (405 nm diode laser) at 100% laser power for 36 iterations (frame average: 6, line average: 6) using the normal imaging setting on the Leica SP8 HyD detector system. An image was taken of each embryo prior to photoconversion with the excitation light of 488 nm (490–550 nm) or 552 nm (580-670) HyD lasers set at 30% laser power for both channels on standard mode. Photoconversion was performed at the time of cytokinesis of the EMS cell, and 2 minutes after cytokinesis the timecourse was started, with 1 minute between each image taken for 7 minutes. DENDRA2::SYS-1 nuclear levels were normalized by N2 values utilizing the same settings described above.

Results

Photobleaching reveals *de novo* and inherited SYS-1 pools in the E and MS cells and centrosomal SYS-1 dynamics over time.

Previous data show changes in centrosomal SYS-1 levels and dynein trafficking correlate with nuclear SYS-1 levels in WβA daughter cells (VORA AND PHILLIPS 2015; THOMPSON *et al.* 2022). Disruption of SYS-1 centrosomal levels by knockdown of the centrosomal scaffold protein RSA-2, different dynein subunits (DHC-1, DLC-1, DYLT-1), or the proteasome trafficking adaptor protein ECPS-1 is sufficient to induce a change in cell fate to a Wnt-signaled cell fate in the distal tip cells and the seam cells (THOMPSON *et al.* 2022). These data suggest that impairing SYS-1 centrosomal localization or degradation increases SYS-1 inheritance in the daughters of mother cells that have impaired SYS-1 degradation capability. However, it remains possible that degradation of SYS-1 in the mother cell is also incomplete in wild type and that inherited SYS-1 contributes to normal Wnt-dependent asymmetric cell fate specification. To better understand the dynamics of SYS-1 inheritance in wild type, we used

fluorescence recovery after photobleaching (FRAP) in the E and MS daughter cells at different time points. The EMS cell is polarized by Wnt ligand produced in the posterior P2 cell, resulting in E and MS daughter cells with high and low nuclear levels of SYS-1, respectively (GOLDSTEIN 1992; HARRELL AND GOLDSTEIN 2011; ROBERTSON AND LIN 2012). The EMS cell was photobleached at different times during mitosis, and the nuclear levels in the E and MS daughter cells were measured (Fig. 1A). Specifically, EMS was photobleached at anaphase, telophase, and cytokinesis and the levels of nuclear SYS-1 in the resulting daughter cells was quantified at four minutes after cytokinesis (Fig. 1B). If SYS-1 is cleared by the mother cell centrosomal processing, we expect no differences between SYS-1 nuclear levels due to EMS photobleaching at different timepoints. Alternatively, if the mother cell SYS-1 protein is inherited by the daughter cells, we expect the largest decrease in SYS-1 levels to occur following the photobleach at cytokinesis. Anaphase photobleach gives slight, non-significant decrease (Fig 1B), but we speculated that this result may be due to SYS-1 synthesis later during mitosis, giving rise to an unbleached population of mother cell SYS-1. To address this, we repeated the photobleaching experiment at telophase and at cytokinesis. Indeed, after the EMS telophase photobleach, we observed significant decreases in E and MS nuclear SYS-1, suggesting the degradation of SYS-1 is incomplete in the mother EMS cell (Fig. 1B). Finally, due to the possibility of late cell cycle SYS-1 synthesis, we photobleached at cytokinesis to rule out mother cell contribution to daughter cell signal. Despite the late timing of the photobleaching, GFP::SYS-1 was still visible in both daughter cell nuclei, revealing both a mother cell contribution and a *de novo* synthesized SYS-1 pool in the E and the MS daughter cells (Fig. 1B). Regardless of the time of photobleaching, the asymmetry between E and MS SYS-1 nuclear levels is maintained (Fig. 1B). These results suggest SYS-1 mother cell clearance is incomplete and that *de novo* SYS-1 is asymmetrically regulated during EMS ACD.

To observe the dynamics of the *de novo* SYS-1 pool in the daughter cells, we photobleached the EMS mother cell at cytokinesis and measured *de novo* and total nuclear SYS-1 at different times (4, 6, 8, and 10 mins after cytokinesis). We measured SYS-1 levels of the E and MS cells at different times with and without photobleaching at cytokinesis to determine the effect of the EMS cell cycle on total and *de novo* SYS-1 accumulation over time. Because *de novo* nuclear SYS-1 levels were reduced by 45–83%

relative to the total levels at each time point, our results suggest SYS-1 inheritance occurs in wild type from the EMS into the E and MS daughter cells and that photobleaching at cytokinesis has a measurable effect on SYS-1 levels throughout the daughter cell cycle.

Interestingly, the accumulation of *de novo* SYS-1 was not linear. Instead, we observed a significant increase in nuclear *de novo* SYS-1 levels in both daughter cells during minutes four through six, as expected given the time needed for new synthesis (Fig. 1C). However, *de novo* SYS-1 levels plateau around 8 min and then decrease at 10 min, after cytokinesis of the mother cell (Fig. 1C), suggesting *de novo* SYS-1 accumulation changes throughout the cell cycle. To quantify this change, we calculated the ratio of total to *de novo* nuclear SYS-1 levels over the timecourse in both daughter cells. In the E cell at four minutes, the *de novo* SYS-1 pool represents about one-third (Fig. 1D, 4 min=28.9%) of the total SYS levels and increases to roughly half (6 min=54.2%; 8 min=51.5%) by minutes 6–8 after mother cell division. Ten minutes after cytokinesis *de novo* SYS-1 decreases to 33%. We observe a similar pattern in the MS cell (4 min=17%; 6 min=45%; 8 min=50%; 10 min=29%), though the absolute levels are higher in the Wnt-signaled E daughter (Fig. 1C). This timecourse revealed variable rates of *de novo* SYS-1 synthesis and regulation in the nuclei of the E and MS daughter cells through the cell cycle, suggesting the role of Wnt signaling in SYS-1 stabilization is mostly complete by 8 minutes post-EMS division and, surprisingly, that the “unsignaled” MS cell also stabilizes SYS-1, albeit at a lower level than E.

<u>Photoconversion of DENDRA2::SYS-1 reveals turnover at the centrosome during mitosis.</u>

To visualize *de novo* and inherited SYS-1, we generated a photoconvertible *sys-1* transgene, P_{sys-1}::DENDRA2::SYS-1. With this new tool, we were able to observe and differentiate preexisting (red) and newly synthesized (green) SYS-1 centrosomal accumulation in the P1 cell, which has been previously utilized for SYS-1 centrosomal localization and processing studies (VORA AND PHILLIPS 2015; THOMPSON *et al.* 2022). While observing P1 cellular division, in the green channel DENDRA2::SYS-1 is visible at the centrosome prior to photoconversion, consistent with previous studies (VORA AND PHILLIPS 2015; THOMPSON *et al.* 2022) (Fig. 2A), while the red channel detection shows a lack of DENDRA2::SYS-1 at the centrosomes (Fig. 2B). To photoconvert DENDRA2::SYS-1 from green to red fluorescence, we

exposed the entire P1 cell to a UV laser (405nm diode laser) (CHUDAKOV *et al.* 2007) at 100% laser power for 36 iterations. After photoconversion, centrosomal DENDRA2::SYS-1 in the green channel sharply decreases (Fig. 2C) and we clearly detect red fluorescent DENDRA2::SYS-1 at the centrosome (Fig. 2D). After confirming successful photoconversion, we measured centrosomal DENDRA2::SYS-1 levels in 20-second increments through P1 mitosis (Fig. 2E). The raw data revealed the preexisting, red centrosomal DENDRA2::SYS-1 decreased over time, likely due to centrosomal degradation. Interestingly, the newly synthesized, green centrosomal DENDRA2::SYS-1 decreased at a slower rate throughout the rest of P1 mitosis (Fig. 2E). This suggests the rate of synthesis and trafficking is relatively equal to the rate of degradation of *de novo* SYS-1 at the centrosome, which is consistent with the previously published idea of a steady-state level of centrosomal GFP::SYS-1 that is stable during the P1 cell mitosis (Vora and Phillips, 2015).

To specifically evaluate the enrichment of DENDRA2::SYS-1 at the centrosome, we used the centrosomal enrichment index (CEI) (THOMPSON *et al.* 2022). The CEI allows us to measure the degree to which the mother cell traffics SYS-1 to the centrosome, thus enriching SYS-1 fluorescence at the centrosome, while also internally controlling for bleaching via repetitive imaging. The CEI measurement allowed us to more clearly observe the initial increase in the red channel of centrosomal DENDRA2::SYS-1 after photoconversion (Fig. 2F). The CEI data show a similar rate of declining preexisting DENDRA2::SYS-1 centrosomal levels as the raw data but emphasizes the stability of newly translated centrosomal DENDRA2::SYS-1 enrichment, which is stable and low (Fig. 2F), as cytoplasmic DENDRA2::SYS-1 fluorescence also decreases over time. Since we would expect no centrosomal enrichment of preexisting DENDRA2::SYS-1 if SYS-1 were trafficked to a different locale to be degraded, our finding is consistent with our model of SYS-1 enrichment from the cytoplasm and subsequent degradation at the centrosome.

To further examine the dynamics of centrosomal SYS-1 during the mitotic division of the P1 cell, we photoconverted the anterior centrosome of P1 at early metaphase and quantified both preexisting (red) and newly trafficked (green) DENDRA2::SYS-1 in 20-second increments. We averaged seven biological replicates to quantify the initial amount of pre-conversion centrosomal green DENDRA2::SYS-

1 to normalize centrosomal DENDRA2::SYS-1 measurements and to compare how preexisting and newly synthesized SYS-1 are turned over through mitosis. After photoconversion, we observed an initial increase in newly trafficked green centrosomal DENDRA2::SYS-1 followed by a steady decrease (Fig. 2G). Photoconversion of the entire cell (Fig. 2F) suggests that green, newly synthesized SYS-1 is being replenished via trafficking through mitosis. When we photoconvert only the centrosome, the observed initial increase in the green channel implies active trafficking of SYS-1 to the centrosome early in mitosis followed by a decrease in newly trafficked SYS-1 until a stable steady state is achieved (Fig. 2G), which is consistent with the trafficking model previously observed (THOMPSON *et al.* 2022). Following photoconversion of the anterior P1 centrosome, the amount of red, preexisting photoconverted DENDRA2::SYS-1 slowly decreases during mitosis (Fig. 2G, S1A). Consistent with SYS-1 centrosomal clearance during mitosis (VORA AND PHILLIPS 2015), our data suggest preexisting and newly trafficked SYS-1 are degraded by the centrosomal proteosome. Altogether, these data suggest that newly synthesized and trafficked SYS-1 coupled with degradation of preexisting centrosomal SYS-1 lead to a stable steady state at the centrosomal locale, while indicating that the centrosome is the terminal locale of SYS-1.

Photoconversion of the cytoplasm of the P1 cell unveils dynamics of dynein trafficking of DENDRA2::SYS-1 during mitosis.

Previous data showed that microtubule trafficking via the dynein complex is needed for SYS-1 centrosomal localization (THOMPSON *et al.* 2022) and our centrosome photoconversion data showed an initial increase in newly trafficked SYS-1 suggesting that active transport of SYS-1 is needed to regulate SYS-1 in the daughter cells after ACD (Fig. 2G) . By photoconverting subdomains of the P1 cell cytoplasm, we tested the ability of the cell to traffic SYS-1 to the centrosome. Additionally, we impaired SYS-1 trafficking by knocking down the dynein light chain (DLC-1) of the dynein complex to observe its effect on centrosomal DENDRA2::SYS-1 and better understand SYS-1 trafficking and degradation at the mitotic centrosome. Following initial imaging during early mitosis, where pre-conversion levels of centrosomal DENDRA2::SYS-1 were measured with both green and red emission, a portion of the

cytoplasm was photoconverted (Fig. 3A). After photoconversion, embryos were imaged every 20 seconds during mitosis. Here, due to the directionality of SYS-1 localization and degradation, we predict the older pre-existing centrosomal DENDRA2::SYS-1 would be observable by green emission while the newly trafficked centrosomal SYS-1 would be observable by red emission (i.e., the opposite of fig. 2G). We expect to see an initial increase, due to active trafficking during early mitosis followed by a sharp decrease in the pre-existing, green DENDRA2::SYS-1 at the centrosome, while the newly trafficked, red DENDRA2::SYS-1 will remain more stable through mitosis because it is continuously replenished via dynein trafficking. As expected, the CEI of control *lacZ*(RNAi) embryos, showed pre-existing, green DENDRA2::SYS-1 levels at the centrosome increase soon after photoconversion of the cellular cytoplasm—which is consistent with active trafficking of cytoplasmic SYS-1 to the centrosome via dynein interaction (THOMPSON *et al.* 2022)—followed by a steep decrease as this older population of SYS-1 is degraded (Fig. 3B). Meanwhile, following cytoplasmic photoconversion, newly trafficked DENDRA2::SYS-1 levels at the centrosome initially increase and are then relatively stable and enriched compared to the cytoplasm throughout the post-conversion timecourse. These data suggest turnover of centrosomal SYS-1 is balanced by new trafficking of newly trafficked SYS-1 from the cytoplasm to the centrosome (Fig. 3B).

To observe the impact of microtubule trafficking on DENDRA2::SYS-1, we knocked down the light subunit of the dynein complex, DLC-1, via RNAi feeding. Previous results show DLC-1 is required for efficient centrosomal enrichment of SYS-1 (THOMPSON *et al.* 2022). After *dlc-1(RNAi),* the red, newly trafficked DENDRA2::SYS-1 is more stable throughout mitosis; however, newly trafficked SYS-1 is present at lower levels than in the control (Fig. 3C). This result is consistent with impaired SYS-1 centrosomal recruitment observed in cells lacking efficient dynein trafficking (THOMPSON *et al.* 2022). To better observe the dynamics of the newly trafficked DENDRA2::SYS-1, Figure 3D directly compares control embryos to embryos with depleted DLC-1. DLC-1 knockdown hinders SYS-1 trafficking to the centrosome, resulting in a decrease of centrosomal SYS-1 enrichment throughout mitosis compared to controls (Fig. 3D). These data, which is consistent with our model of SYS-1 degradation by the centrosomal proteasome, suggests microtubule trafficking via the dynein complex is key for centrosomal

SYS-1 localization. Notably, degradation is sequential as pre-existing SYS-1 at the centrosome is degraded prior to the newly trafficked SYS-1 which is stably replenished by cytoplasmic trafficking dependent on dynein.

E and MS inheritance of mother cell SYS-1 is limited by EMS centrosomal processing.

To determine the extent to which changes in SYS-1 centrosomal trafficking and degradation affect inheritance of mother cell SYS-1 into the daughter cells, we photoconverted the entire EMS cell of DENDRA-2::SYS-1-expressing embryos at cytokinesis and measured inherited (red) SYS-1 in the E and MS daughter cell nuclei. As the first ACD driven by the Wnt/β-catenin asymmetry pathway, we specifically analyzed the EMS cell division (HARRELL AND GOLDSTEIN 2011). Here, the E cell is the Wnt-signaled cell that normally exhibits higher SYS-1 levels, and the MS daughter is the unsignaled cell with lower SYS-1 levels (HUANG *et al.* 2007; PHILLIPS *et al.* 2007). For photoconversion of DENDRA2::SYS-1, we exposed the whole EMS cell to a UV laser (405nm diode laser) (CHUDAKOV *et al.* 2007) at 100% laser power for 36 iterations during cytokinesis of the EMS cell. Subsequently, we waited two minutes for the nuclear envelope of the E and MS daughters to reform and imaged every 60 seconds for 7 minutes. Then, we normalized the nuclear fluorescence of DENDRA2::SYS-1 to the nuclear autofluorescence in wild-type (N2) embryos using identical measurements. Consistent with our FRAP studies, we observed inherited DENDRA2::SYS-1 present in into both E and MS daughter cells (Fig. 4A). Interestingly, the amount of DENDRA2::SYS-1 inherited by the E daughter was higher than that inherited by the MS cell (Fig. 4A), perhaps reflecting greater stability of inherited SYS-1 in the signaled E cell. We also noted that MS inheritance, while lower than E, was on average above autofluorescence. This result indicates SYS-1 inheritance persists even in the unsignaled MS cell. The timecourse also allowed us to observe changes in nuclear DENDRA2::SYS-1 over the cell cycle of the E and MS cells, up to 9 minutes after EMS division. For both the E and MS daughter cells, we found inherited nuclear DENDRA2::SYS-1 levels to remain stable throughout the timecourse (Fig. 4A). This result indicates the asymmetry in inherited nuclear DENDRA2::SYS-1 occurs shortly after EMS division.

Next, we tested the requirement for dynein trafficking and centrosomal localization in SYS-1 inheritance. We predicted that impaired mother cell SYS-1 processing would lead to an increase in inherited SYS-1 levels, given the previously observed changes in cell fate under these conditions (DLC-1, RSA-2 and ECPS-1 knockdowns) (THOMPSON *et al.* 2022). We observed that when microtubule trafficking is impaired by the knockdown of DLC-1 there is a significant increase in the amount of inherited DENDRA2::SYS-1 nuclear levels of both the E and MS cells (Fig. 4B). Initial levels of inherited SYS-1 were 3 and 10-fold higher in the E and MS cells, respectively (Fig. 4B). These data suggest mother cell dynein trafficking is required to limit the amount of inherited SYS-1.

We further investigated the role of SYS-1 centrosomal localization in controlling SYS-1 inheritance by preventing centrosomal localization of SYS-1 via knockdown of the centrosomal scaffold protein RSA-2. RSA-2 provides a necessary centrosomal scaffold and acts as a direct binding partner for SYS-1 localization at the mitotic centrosome (VORA AND PHILLIPS 2015). Loss of centrosomal localization by *rsa-2(RNAi)* increased the amount of inherited nuclear DENDRA2::SYS-1 by 3.4- and 11-fold in E and MS daughter cells, respectively (Fig. 4C). Lastly, we impaired the degradation of centrosomal SYS-1 by knocking down the adaptor protein ECPS-1, the worm homolog to EMC29, (a proteasome-dynein adaptor and scaffold (LEGGETT *et al.* 2002; LEHMANN *et al.* 2010). Previous studies showed that ECPS-1 knockdown leads to an increase of SYS-1 levels at the centrosome, suggesting its role in SYS-1 centrosomal degradation (THOMPSON *et al.* 2022). *ecps-1*(RNAi) lead to an increase of the amount of DENDRA2::SYS-1 inherited into the E and MS cells by 3- and 10.7-fold, respectively (Fig. 4D). These data suggest that ECPS-1 knockdown impairs degradation of SYS-1 in the centrosome of the mother cell and that ECPS-1 function is normally required to prevent SYS-1 over-inheritance.

Finally, to assess the effect of the over-inherited SYS-1 on loss of daughter cell SYS-1 asymmetry and further loss of the asymmetric cell division of EMS, we averaged the inherited DENDRA2::SYS-1 nuclear levels in each condition throughout the 7-minute timecourse and measured the fold change between the E and the MS daughters. These data showed a loss of asymmetry of inherited SYS-1 in all the experimental conditions tested compared to control RNAi (Fig. 4E). The data suggest that, in wild-type conditions, SYS-1 is inherited into both the E and the MS daughter cells, and

that early in the cell cycle, the asymmetry between E and MS is established. For proper inheritance of SYS-1 during the EMS ACD the mother cell requires SYS-1 centrosomal trafficking, coupling, and degradation (also referred to as centrosomal processing) to prevent over-inheritance of SYS-1 and loss of sister cell asymmetry, seen by a reduction in the P:A ratio after loss of centrosomal SYS-1 processing (Fig 4E).

Loss of centrosomal SYS-1 results in increased levels of nuclear *de novo* SYS-1 in EMS daughter cells.

Previously, we showed that loss of trafficking, centrosomal coupling or degradation of SYS-1 leads to higher SYS-1 levels in the daughter cells (Fig. 4) (VORA AND PHILLIPS 2015; THOMPSON *et al.* 2022), which can in turn lead to a loss off the asymmetric cell division (THOMPSON *et al.* 2022). Given the fact that centrosomal processing functions in the mother cell to control over inheritance, we predicted that mother cell, but not *de novo* translated DENDRA2::SYS-1 would be affected when mother cell centrosomal processing of SYS-1 is impaired. To test this, we first measured green/*de novo* DENDRA2::SYS-1 nuclear levels in the E and MS daughter cell over time starting 2 minutes after cytokinesis and in 60 second increments for 7 minutes (Fig. 5A). We observed that both the E cell, the Wnt-signaled cell, and MS, the unsignaled cell, were actively translating DENDRA2::SYS-1 (Fig. 5A), consistent with our FRAP results (Fig.1C). The E cell also showed higher levels of *de novo* nuclear DENDRA2::SYS-1 levels than the MS cell (3.6-fold increase in E vs MS), indicating robust asymmetry in synthesis or stability of newly translated DENDRA2::SYS-1 (Fig. 5A). Additionally, the timecourse showed that the E and MS *de novo* nuclear DENDRA2::SYS-1 levels remained stable (Fig. 5A). These data suggest that SYS-1 synthesis occurs in both the signaled E and unsignaled MS daughter cells and that the synthesis/maintenance rates are higher in E than MS.

Subsequently, we observed *de novo* nuclear DENDRA2::SYS-1 levels in the daughter cells after knocking down DLC-1, therefore impairing microtubule trafficking of SYS-1 to the centrosome in the mother cell (THOMPSON *et al.* 2022). This surprisingly resulted in a significant increase in the amount of *de novo* nuclear SYS-1 levels in both daughter cells at all time points (Fig. 5B). This increase in *de novo* SYS-1 was also observed in the other tested conditions that showed increased DENDRA2::SYS-1

inheritance, *rsa-2* and *ecps-1 (*RNAi) (Fig. 5C and D). In all the tested conditions (*dlc-1, rsa-2* and *ecps-1 (*RNAi)), we also observed a loss of asymmetry compared to the control (Fig. 5E).

Thus, we find that impairing proper SYS-1 centrosomal processing during mitosis of the EMS cell showed increased levels of both inherited and *de novo* nuclear DENDRA2::SYS-1 in EMS daughter cells (Fig. 4B,C,D and Fig. 5B,C,D). Additionally, we observed that over time in the tested conditions, nuclear DENDRA2::SYS-1 consistently decreases in backgrounds with higher than normal SYS-1 compared to wild type, which stably maintains its SYS-1 levels in E and MS (Fig. 4B, C,D and Fig. 5B,C,D) (Table 1). This pattern of increased rate of DENDRA2::SYS-1 loss was observed in both DENDRA2::SYS-1 pools, suggesting that both pools, *de novo* and inherited, in the E and MS cells are processed similarly. These data suggest that over-inheritance of SYS-1 during asymmetric cell division affects the *de novo* SYS-1 that is generated or maintained in both daughter cells. This led us to hypothesize that the β-catenin "destruction complex" activity in daughter cells has a limited capacity and is not fully able to regulate SYS-1 properly in situations with increased levels of inherited SYS-1, an idea we test below.

<u>Partial loss of the negative regulator of the Wnt signaling pathway, APR-1, affects both pools of nuclear SYS-1 in the E and MS cells.</u>

To investigate the role of the destruction complex in regulating *de novo* and inherited SYS-1 during asymmetric cell division and during the cell cycle of the E and MS daughter cells we impaired a SYS-1 negative regulator of the Wnt pathway, APR-1 (HUANG *et al.* 2007; BALDWIN AND PHILLIPS 2014). APR-1 is a homolog of vertebrate APC, which is part of the β-catenin destruction complex and functions to limit β-catenin cytoplasmic accumulation in the Wnt-unsignaled state. APC/APR-1 also limits Wnt pathway activity after initial activation by targeting β-catenin for proteasomal degradation (CLEVERS AND NUSSE 2012). As expected, we found that partial depletion of APR-1 via RNAi feeding led to a significant increase in *de novo* DENDRA2::SYS-1 nuclear levels throughout the MS cell cycle (Fig. 6A). We also observed a 2-fold increase in *de novo* DENDRA2::SYS-1 during the E cell cycle (Fig. 6A), which has not been shown previously. This result was unexpected as a role of APR-1 as a negative regulator of SYS-1 had been primarily observed in the unsignaled MS cell (HUANG *et al.* 2007; SUGIOKA *et al.* 2011; BALDWIN

AND PHILLIPS 2014; BALDWIN *et al.* 2016), while these data suggest APR-1 regulates SYS-1 levels in both daughter cells.

Additionally, we observe different nuclear DENDRA2::SYS-1 dynamics when APR-1 is knocked down compared to other backgrounds with elevated *de novo* DENDRA2::SYS-1. The E and MS cells *de novo* DENDRA2::SYS-1 levels show a smaller decrease compared to the DLC-1, RSA-2, and ECPS-1 knockdowns (Table 1), over the 7-minute timecourse (Fig. 6A). These results suggest that *de novo* SYS-1 in both daughter cells is limited by the destruction complex in wild type and in situations with elevated inherited SYS-1.

We proceeded to quantify the changes in inherited DENDRA2::SYS-1 nuclear levels in the E and MS on *apr-1(*RNAi), to observe the effect of increasing the *de novo* pool directly has on the inherited SYS-1 pool. We observed increased levels of inherited nuclear SYS-1 in both daughter cells (Fig. 6B). Consistent with previous observations in which APR-1 levels are higher in the MS cell (HUANG *et al.* 2007; SUGIOKA *et al.* 2011); we observed the biggest fold change of *de novo* nuclear DENDRA2::SYS-1 in *apr-1(RNAi)* in the MS cell compared to wild type (Fig. 6C). In MS, the *de novo* pool was more highly affected by loss of APR-1 than the inherited pool, suggesting that, in wild type, APR-1 more highly negatively regulates *de novo* DENDRA2::SYS-1 in the MS cell (Fig. 6C). Though the effect of APR-1 depletion on inherited SYS-1 in MS leads to an average of 3.1-fold increase compared to wild type; this was less than the 7.9-fold increase we see in the MS *de novo* SYS-1 pool. By contrast, the difference between E inherited and E *de novo* SYS-1 after APR-1 depletion is not as striking (1.4-fold and 2.3-fold increase compared to wild type, respectively) (Fig. 6C).

Overall, while we do see an effect of APR-1 regulation of SYS-1 in the E daughter cell, the fold change of DENDRA2::SYS-1 nuclear *de novo* levels is not as drastic in E compared to MS, where we observe a nearly 8-fold increase in the newly translated SYS-1 on *apr-1(*RNAi) (Fig. 6C). Therefore, the major regulatory function of APR-1 on SYS-1 nuclear levels in EMS ACD is to limit accumulation of *de novo* SYS-1 in MS.

Despite the decreased effect of APR-1 depletion on DENDRA2::SYS-1 nuclear levels in E, our results suggest that APR-1 is also functioning in this Wnt-signaled daughter cell. However, an alternative

hypothesis explaining our increased SYS-1 levels in E after APR-1 depletion is that APR-1 negatively regulates SYS-1 earlier in the EMS lineage. In this case, increased SYS-1 inheritance is would be expected to increase the total SYS-1 levels and possibly the stability of *de novo* SYS-1 in the daughter cells. To distinguish between these possibilities, we knocked down APR-1 and observed changes in total centrosomal DENDRA2::SYS-1 levels in the EMS cell during mitosis with no photoconversion. Centrosomal SYS-1 quantitation is a good readout of SYS-1 levels in the EMS cell and its progenitors because SYS-1 centrosomal accumulation reflects cytoplasmic SYS-1 levels (VORA AND PHILLIPS 2015) and any effect of SYS-1 levels can be clearly observed immediately before the cell divides, providing the latest timepoint possible before the birth of E and MS. We found that there is no significant change in centrosomal DENDRA2::SYS-1 levels in the EMS cell on *apr-1(RNAi)* compared to wild type (Fig. 6D), suggesting SYS-1 is not negatively regulated by APR-1 in EMS or its progenitors. Thus, our observations suggest that when the inherited SYS-1 pool is affected in the EMS mother cell, the *de novo* SYS-1 pools are secondarily affected in the daughter cells. However, our data indicates there is free exchange between these pools which means that the opposite is also true: increasing *de novo* SYS-1 increases the observed level of inherited SYS-1, likely through increasing its stability (see discussion). Additionally, here we observed a role for APR-1 limiting the accumulation of both SYS-1 pools in both the signaled and unsignaled EMS daughter cells.

Discussion

In *C. elegans,* successful asymmetric cell divisions throughout development depend on proper regulation of SYS-1 levels. Here we show that in wild-type conditions, proper SYS-1 centrosomal degradation in the EMS mother cell is key to regulate inheritance into the E and MS cells during ACD. It was previously established that SYS-1 centrosomal trafficking, coupling and degradation in the mother cell is key for regulation of limiting subsequent daughter cell SYS-1 levels and subsequent asymmetric cell fate specification (VORA AND PHILLIPS 2015; THOMPSON *et al.* 2022). These data suggested SYS-1 inheritance was normally limited by centrosomal degradation and that *de novo* synthesized SYS-1, regulated by asymmetric Wnt pathway activity, was the source of nuclear SYS-1 important for ACD.

However, SYS-1 inheritance (or the lack thereof) and the role of centrosomal degradation have not been demonstrated. Photobleaching experiments show that mother cell bleaching of GFP::SYS-1 decreases the total GFP::SYS-1 in the daughter cells, suggesting that inherited SYS-1 was present in daughter cell nuclei in wild-type conditions. DENDRA2::SYS-1 photoconversion at cytokinesis directly confirmed DENDRA2::SYS-1 inheritance to both the E and the MS cell and that loss of centrosomal SYS-1 degradation not only increases the inherited DENDRA2::SYS-1 pool but also unexpectedly increases/stabilizes the *de novo* synthesized pool. We show that APR-1 regulates both inherited and *de novo* SYS-1 in E and MS, and the rate of clearance of extra inherited SYS-1 is dependent on APR-1 function. Photoconvertible SYS-1 also allowed us to test the model of SYS-1 trafficking to its final destination in the cell, the mitotic centrosome. Photoconversion of DENDRA2::SYS-1 at the centrosome during metaphase demonstrated that newly synthesized DENDRA2::SYS-1 is continually trafficked to the centrosome during mitosis, resulting in stable steady state SYS-1 levels despite this localization leading to increased SYS-1 turnover (VORA AND PHILLIPS 2015). In contrast, preexisting SYS-1 is more enriched at the centrosome and decreases through mitosis. Thus, proper SYS-1 levels are dependent on both trafficking and degradation of SYS-1 in the mother cell along with negative regulation via the destruction complex in the daughter cells.

Therefore, we proposed the following model (Fig 7). 1) In wild-type conditions during ACD, in the EMS cell, SYS-1 is trafficked to the centrosome where SYS-1 degradation is promoted by the centrosomal proteosome, while the remaining cytoplasmic SYS-1 is inherited into the E and MS daughter cells where it is regulated by the APR-1 (Fig. 7A), primarily (but not exclusively) in MS. *De novo* SYS-1 also accumulates in the daughter cells, but this pool is regulated similarly as the inherited pool. 2) Loss of mother cell regulation of centrosomal SYS-1 levels via depletion of RSA-2, DLC-1 or ECPS-1 prevents proper degradation of mother cell SYS-1 leading to over-inheritance of SYS-1 in both daughter cells. A higher rate of SYS-1 inheritance correlated with higher *de novo* SYS-1 levels in both daughter cells, indicating an inability of the destruction complex to effectively regulate both SYS-1 pools due to dilution of the destruction complex activity (Fig. 7B). 3) Loss of the negative regulator APR-1 has a direct effect in the *de novo* levels in both the E and the MS cells as we see no effect on EMS mother cell SYS-1 levels.

Due to the similar regulation of *de novo* SYS-1 and inherited SYS-1 pools by APR-1, increased levels of *de novo* SYS-1 in turn lead to an apparent increase in inherited SYS-1, likely due to increased stability of this pool. A loss of APR-1 therefore leads to increased total SYS-1 levels and a loss of daughter cell asymmetry (Fig. 7C).

Are the rates of trafficking and degradation of centrosomal SYS-1 in the mother cell similar?

While investigating DENDRA2::SYS-1 trafficking, when photoconverting the P1 cell during early metaphase, our results showed that preexisting SYS-1 (red), was readily degraded at the centrosome while newly synthesized SYS-1 is more stable through mitosis (Fig. 2F &E). This suggests that the rate at which newly synthesized SYS-1 is trafficked to the centrosome is comparable to its rate of degradation, promoting stable levels through mitosis, while preexisting or "older" SYS-1 is more rapidly degraded. Interestingly, this type of dynamics has been observed before. Previous studies showed that centrosomal SYS-1 levels increased as the centrosome assembles, but then is present at a stable steady state for metaphase and much of anaphase. As the centrosome disintegrate, centrosomal localization of SYS-1 was lost (VORA AND PHILLIPS 2015). Later studies showed that microtubule trafficking via the dynein of SYS-1 enhanced its centrosomal localization (THOMPSON *et al.* 2022). In our studies, when we photoconverted a portion of cytosolic DENDRA2::SYS-1 both the proximal and distal centrosome accumulated newly trafficked SYS-1, though photoconverted SYS-1 was observed at higher levels on the proximal centrosome (Fig. S2). These data suggest that free SYS-1 is mobile and can localize to either centrosome. When DLC-1 was partially depleted, the rate of trafficking was diminished and the DENDRA2::SYS-1 that was already at the centrosome was more rapidly depleted (Fig. 3C and D). Altogether, these data suggest that SYS-1 trafficking to the centrosome allows for its continuous degradation by the centrosomal proteosome and the "older" SYS-1 is more likely to be degraded. Additionally, it seems likely that coupling and accumulation of SYS-1 to the centrosome is dependent on pericentriolar material (PCM) assembly and disassembly (VORA AND PHILLIPS 2015), while processing of centrosomal SYS-1 is dependent on proper localization of the proteasome to the centrosome (Fig. 4D, 5D) (THOMPSON *et al.* 2022).

Why do we observe differential levels of inherited SYS-1?

Here we conduct the first examination of SYS-1 inheritance during ACD to test the ability of mother cells to regulate the level of SYS-1 in its daughters. A photoconvertible DENDRA2::SYS-1 under the endogenous promoter enabled the observation and quantification of DENDRA2::SYS-1 inheritance during the ACD of the EMS cell (Fig. 4A). Interestingly, the inherited DENDRA2::SYS-1 is not equal for both daughter cells, E shows higher levels of SYS-1 through the timecourse than its sister MS (Fig. 4A). Previous studies show a strong asymmetry of APR-1 during the EMS cell division, accumulating in the anterior side (SUGIOKA *et al.* 2011; SUGIOKA *et al.* 2018). Our data showed that APR-1 predominantly functions in the MS cell, though we do also see APR-1 depletion effects in E (Fig. 6C). This suggests that SYS-1 inheritance may be symmetric (VORA AND PHILLIPS 2015), or at least correlates with the volume of the cytoplasm, but the stability of SYS-1 is asymmetric in the two daughter cells. In this model, inherited DENDRA2::SYS-1 in wild type condition is more stable and prevalent in the E cell (Fig. 4A). However, it remains feasible that asymmetric inheritance of other Wnt signaling components, such as Frizzled or Dishevelled, contribute to the asymmetry we observed. Indeed, asymmetric MOM-5/Frizzled has been reported in the early embryonic blastomeres (PARK *et al.* 2004) and the seam cells (MIZUMOTO AND SAWA 2007), suggesting these components could be influencing the distribution of other Wnt signaling components during ACD. In mammals, during the ACD of T cells, there is a differential inheritance of two different cell determinants, Numb and α-Adaptin (PHAM *et al.* 2015). The asymmetry observed was due to the presence of CXCR4 signaling and stromal interactions (PHAM *et al.* 2015). A similar mechanism was observed in *D. melanogaster* sensory organ precursors, in which asymmetric inheritance of Numb was key for a successful ACD (ORGOGOZO *et al.* 2002). All together, these data suggest that while SYS-1 might be symmetrically inherited into the daughter cells, further SYS-1 regulation and stability is dependent on the asymmetric inheritance of positive and negative regulators of Wnt-signaling.

Why does over-inheritance of SYS-1 correlate with higher levels of *de novo* SYS-1 levels?

While loss of microtubule trafficking, centrosomal coupling or degradation of SYS-1 in the mother cell led to an increase in the amount of inherited DENDRA2::SYS-1, we also observed increased levels of *de novo* DENDRA-2::SYS-1 in both daughter cells. These unexpected results led to further investigation of the role of negative regulators of SYS-1 in the Wnt-signaling pathway. Since APR-1 depletion primarily affects *de novo* DENDRA2::SYS-1 rather than DENDRA2::SYS-1 levels in the mother cell (Fig 6A, D), we used this background to test the effect of increased *de novo* DENDRA2::SYS-1 on maintenance of the inherited DENDRA2::SYS-1 pool. We observed increased inherited nuclear DENDRA2::SYS-1 levels in both daughter cells (Fig. 6B). These results supported our hypothesis that when either of the pools is affected, this will influence the amount of nuclear SYS-1 in the other pool. These results could be explained by an overwhelming of the destruction complex that is equally targeting both de novo and inherited SYS-1 pools, thus leading to an accumulation of *de novo* SYS-1 as destruction complex activity is diluted by increased inherited SYS-1. Our data suggest that increased levels of SYS-1 in the daughter cells directly increases SYS-1 stability in the primarily affected pool (inherited DENDRA2::SYS-1 in *dlc-1, rsa-2 and ecps-1*(RNAi) or *de novo* DENDRA2::SYS-1 in *apr-1*(RNAi)), which in turn perturbs negative regulation of the other pool, leading to an increase in the total levels of nuclear SYS-1. Thus, we conclude that the SYS-1 pools are interchangeable, and both regulated by the destruction complex.

APR-1 depletion also allowed to test the hypothesis that the rate of nuclear SYS-1 loss observed where we have high levels of inherited DENDRA2::SYS-1 (RSA-2, ECPS-1, or DLC-1 depletion) are due to the function of the destruction complex degradation of SYS-1 back to basal levels. APR-1 knockdown, though causing elevated SYS-1 levels, also led to a more moderate rate of decrease in *de novo* SYS-1 levels throughout the timecourse compared to the other conditions tested (*dlc-1, rsa-2 and ecps-1(RNAi)*), suggesting efficient clearance of extra SYS-1 requires APR-1 (Table1) (Fig. 6A). However, when we observed inherited DENDRA2::SYS-1 on *apr-1* (RNAi) levels still decreased over time. Whether this is due to inherent instability of SYS-1 protein, insufficient knockdown of APR-1 or another SYS-1 degradation mechanism remains elusive.

APR-1 functions in the E cell?

Our data suggest that the destruction complex functions in the Wnt-signaled E cell. When knocking down APR-1, we found increased levels of *de novo* nuclear DENDRA2::SYS-1 in both the E and the MS, and while this result was expected for the MS cell, we did not expect to see significant changes in the E cell (Fig. 6A and B). Previous studies investigated the kinetic responses of β-catenin to Wnt-signaling in mammalian cells and found that the destruction complex functions in both the absence and presence of Wnt-signaling. However, when Wnt ligand is present, the destruction complex is only partially active (HERNÁNDEZ *et al.* 2012). While this has not yet been described, in *C. elegans*, our results support those findings. The FRAP experiments demonstrated that *de novo* GFP::SYS-1 plateaus around 6 to 8 minutes which suggests its stabilization is temporally limited in the E cell (Fig. 1D), and this could be due to function of the destruction complex. Additionally, the partial depletion of APR-1 via RNAi in our experiments seems to lower the steady state of degradation happening when Wnt-signaling is present, which supports the observed role for the destruction complex in the E cell.

While our studies focused on the EMS daughter cells, previous studies showed that in both the daughters of E (Ea and Ep) and MS (MSa and MSp), SYS-1 asymmetry is lost after *apr-1*(RNAi) (HUANG *et al.* 2007). These results further support the idea that APR-1 regulation is key to maintain daughter cell asymmetry and its role in both E, the Wnt-signaled daughter cell and MS, the unsignaled cell. In addition, it has been previously shown that the observed asymmetry is not due to nuclear export or differential subcellular distribution of SYS-1, but to the proteasomal degradation (HUANG *et al.* 2007). These data suggests that SYS-1 asymmetry is tightly regulated by proteasomal degradation via mother cell centrosomal processing and the destruction complex function in the EMS daughters.

Is SYS-1 inheritance the memory mechanism?

We observe that the rate of DENDRA2::SYS-1 clearance increases/scales with higher levels of inherited DENDRA2::SYS-1 resulting in a tendency to return to basal levels over time (Table 1), which suggests that SYS-1 inheritance itself is not causative in the enrichment of SYS-1 observed previously in signaled cousins (ZACHARIAS *et al.* 2015). In addition to SYS-1 cousin enrichment, consistent lineage-

dependent changes in POP-1/TCF and WRM-1/β-catenin levels demonstrate that Wnt signaled daughters of Wnt signaled cells respond more strongly to Wnt signaling in subsequent divisions compared to their cousins that have fewer Wnt signaled cells in their lineage (ZACHARIAS *et al.* 2015; ZACHARIAS AND MURRAY 2016). The observed enrichment in signaling status could be due to the asymmetric localization or activation of upstream Wnt pathway components, including the Frizzled receptor or the Dishevelled scaffold protein, which have been observed to be asymmetrically localized in Wnt-dependent ACDs in the early embryo (PARK *et al.* 2004) and the seam lineage (MIZUMOTO AND SAWA 2007; BALDWIN AND PHILLIPS 2014; SUGIOKA *et al.* 2018). A continued asymmetric inheritance over multiple ACDs might then lead to skewed activation/accumulation of other Wnt pathway components. In addition, this model cannot exclude the biased inheritance of post-translational modification states, such as phosphorylation, and their effect on SYS-1 or other proteins that regulate Wnt activity (ZACHARIAS *et al.* 2015)(Zacharias *et al*., 2015). Together, these data suggest that though proper regulation of SYS-1 inheritance, as well as context-dependent regulation of inherited SYS-1 in daughters, are key for a successful ACD and acquisition of different cell fates, SYS-1 inheritance itself is unlikely to be the basis for the "memory", that allows cell that have been repeatedly signaled to enrich SYS-1 in the nucleus.

Our proposed mechanism of SYS-1 regulation and inheritance during ACD sheds light into how tightly regulated ACD processes are and the several layers of negative regulation needed for proper SYS-1 nuclear levels in the daughter cells and further target gene activation. Indeed, trafficking and degradation of mother cell SYS maintains asymmetric SYS-1 levels in the daughters at a level that can be effectively regulated by the destruction complex.

Acknowledgments

We thank Kimberly Bekas, Emily Hirsh and Amy Clemons for critical thinking and comments on the manuscript. Strains were provided by the Caenorhabditis Genetics Center, which is funded by the National Institutes of Health (NIH) Office of Research Infrastructure Programs (P40 OD01440). We also want to thank the Carver Center for Imaging in the Biology department of the University of Iowa and its director, Dr. Michael Dailey. This work was supported by NIH award GM114007 (to B.T.P), the Graduate

College Post-Comprehensive Research Fellowship and the Graduate College Summer Fellowship to M.V.

References

Bajaj, J., B. Zimdahl and T. Reya, 2015 Fearful symmetry: subversion of asymmetric division in cancer development and progression. Cancer Res 75**:** 792-797.

Baldwin, A. T., A. M. Clemons and B. T. Phillips, 2016 Unique and redundant β-catenin regulatory roles of two Dishevelled paralogs during C. elegans asymmetric cell division. J Cell Sci 129**:** 983-993.

Baldwin, A. T., and B. T. Phillips, 2014 The tumor suppressor APC differentially regulates multiple β-catenins through the function of axin and CKIα during C. elegans asymmetric stem cell divisions. J Cell Sci 127**:** 2771-2781.

Barth, A. I., H. Y. Caro-Gonzalez and W. J. Nelson, 2008 Role of adenomatous polyposis coli (APC) and microtubules in directional cell migration and neuronal polarization. Semin Cell Dev Biol 19**:** 245-251.

Bekas, K. N., and B. T. Phillips, 2020 Generating reliable hypomorphic phenocopies by RNAi using long dsRNA as diluent. MicroPubl Biol 2020.

Brenner, S., 1974 The genetics of Caenorhabditis elegans. Genetics 77**:** 71-94.

Chen, G., S. Yin, H. Zeng, H. Li and X. Wan, 2022 Regulation of Embryonic Stem Cell Self-Renewal. Life (Basel) 12.

Chhabra, S. N., and B. W. Booth, 2021 Asymmetric cell division of mammary stem cells. Cell Div 16**:** 5.

Christian, J. L., 2012 Morphogen gradients in development: from form to function. Wiley Interdiscip Rev Dev Biol 1**:** 3-15.

Chudakov, D. M., S. Lukyanov and K. A. Lukyanov, 2007 Using photoactivatable fluorescent protein Dendra2 to track protein movement. Biotechniques 42**:** 553, 555, 557 passim.

Clevers, H., and R. Nusse, 2012 Wnt/β-catenin signaling and disease. Cell 149**:** 1192-1205.

Conte, D., Jr., L. T. MacNeil, A. J. M. Walhout and C. C. Mello, 2015 RNA Interference in Caenorhabditis elegans. Curr Protoc Mol Biol 109**:** 26.23.21-26.23.30.

de la Roche, M., J. Worm and M. Bienz, 2008 The function of BCL9 in Wnt/beta-catenin signaling and colorectal cancer cells. BMC Cancer 8**:** 199.

Giles, R. H., J. H. van Es and H. Clevers, 2003 Caught up in a Wnt storm: Wnt signaling in cancer. Biochim Biophys Acta 1653**:** 1-24.

Goldstein, B., 1992 Induction of gut in Caenorhabditis elegans embryos. Nature 357**:** 255-257.

Habib, S. J., and S. P. Acebrón, 2022 Wnt signalling in cell division: from mechanisms to tissue engineering. Trends Cell Biol 32**:** 1035-1048.

Harrell, J. R., and B. Goldstein, 2011 Internalization of multiple cells during C. elegans gastrulation depends on common cytoskeletal mechanisms but different cell polarity and cell fate regulators. Dev Biol 350**:** 1-12.

Hayat, R., M. Manzoor and A. Hussain, 2022 Wnt signaling pathway: A comprehensive review. Cell Biol Int 46**:** 863-877.

Hernández, A. R., A. M. Klein and M. W. Kirschner, 2012 Kinetic responses of β-catenin specify the sites of Wnt control. Science 338**:** 1337-1340.

Huang, S., P. Shetty, S. M. Robertson and R. Lin, 2007 Binary cell fate specification during C. elegans embryogenesis driven by reiterated reciprocal asymmetry of TCF POP-1 and its coactivator beta-catenin SYS-1. Development 134**:** 2685-2695.

Kamath, R. S., A. G. Fraser, Y. Dong, G. Poulin, R. Durbin *et al.*, 2003 Systematic functional analysis of the Caenorhabditis elegans genome using RNAi. Nature 421**:** 231-237.

Kidd, A. R., 3rd, J. A. Miskowski, K. R. Siegfried, H. Sawa and J. Kimble, 2005 A beta-catenin identified by functional rather than sequence criteria and its role in Wnt/MAPK signaling. Cell 121**:** 761-772.

Kochendoerfer, A. M., F. Modafferi and E. M. Dunleavy, 2021 Centromere function in asymmetric cell division in Drosophila female and male germline stem cells. Open Biol 11**:** 210107.

Lam, A. K., and B. T. Phillips, 2017 Wnt Signaling Polarizes C. elegans Asymmetric Cell Divisions During Development. Results Probl Cell Differ 61**:** 83-114.

Leggett, D. S., J. Hanna, A. Borodovsky, B. Crosas, M. Schmidt *et al.*, 2002 Multiple associated proteins regulate proteasome structure and function. Mol Cell 10**:** 495-507.

Lehmann, A., A. Niewienda, K. Jechow, K. Janek and C. Enenkel, 2010 Ecm29 fulfils quality control functions in proteasome assembly. Mol Cell 38**:** 879-888.

Lin, R., R. J. Hill and J. R. Priess, 1998 POP-1 and anterior-posterior fate decisions in C. elegans embryos. Cell 92**:** 229-239.

Lo, M. C., F. Gay, R. Odom, Y. Shi and R. Lin, 2004 Phosphorylation by the beta-catenin/MAPK complex promotes 14-3-3-mediated nuclear export of TCF/POP-1 in signal-responsive cells in C. elegans. Cell 117**:** 95-106.

MacDonald, B. T., K. Tamai and X. He, 2009 Wnt/beta-catenin signaling: components, mechanisms, and diseases. Dev Cell 17**:** 9-26.

Mizumoto, K., and H. Sawa, 2007 Cortical beta-catenin and APC regulate asymmetric nuclear beta-catenin localization during asymmetric cell division in C. elegans. Dev Cell 12**:** 287-299.

Morrison, S. J., and J. Kimble, 2006 Asymmetric and symmetric stem-cell divisions in development and cancer. Nature 441**:** 1068-1074.

Neumüller, R. A., and J. A. Knoblich, 2009 Dividing cellular asymmetry: asymmetric cell division and its implications for stem cells and cancer. Genes Dev 23**:** 2675-2699.

Obrador-Hevia, A., S. F. Chin, S. González, J. Rees, F. Vilardell *et al.*, 2010 Oncogenic KRAS is not necessary for Wnt signalling activation in APC-associated FAP adenomas. J Pathol 221**:** 57-67.

Orgogozo, V., F. Schweisguth and Y. Bellaïche, 2002 Binary cell death decision regulated by unequal partitioning of Numb at mitosis. Development 129**:** 4677-4684.

Park, F. D., J. R. Tenlen and J. R. Priess, 2004 C. elegans MOM-5/frizzled functions in MOM-2/Wnt-independent cell polarity and is localized asymmetrically prior to cell division. Curr Biol 14**:** 2252-2258.

Peel, N., M. Dougherty, J. Goeres, Y. Liu and K. F. O'Connell, 2012 The C. elegans F-box proteins LIN-23 and SEL-10 antagonize centrosome duplication by regulating ZYG-1 levels. J Cell Sci 125**:** 3535-3544.

Pham, K., R. Shimoni, M. Charnley, M. J. Ludford-Menting, E. D. Hawkins *et al.*, 2015 Asymmetric cell division during T cell development controls downstream fate. J Cell Biol 210**:** 933-950.

Phillips, B. T., A. R. Kidd, 3rd, R. King, J. Hardin and J. Kimble, 2007 Reciprocal asymmetry of SYS-1/beta-catenin and POP-1/TCF controls asymmetric divisions in Caenorhabditis elegans. Proc Natl Acad Sci U S A 104**:** 3231-3236.

Phillips, B. T., and J. Kimble, 2009 A new look at TCF and beta-catenin through the lens of a divergent C. elegans Wnt pathway. Dev Cell 17**:** 27-34.

Polakis, P., 2012 Wnt signaling in cancer. Cold Spring Harb Perspect Biol 4.

Qu, Y., N. Gharbi, X. Yuan, J. R. Olsen, P. Blicher *et al.*, 2016 Axitinib blocks Wnt/β-catenin signaling and directs asymmetric cell division in cancer. Proc Natl Acad Sci U S A 113**:** 9339-9344.

Quyn, A. J., P. L. Appleton, F. A. Carey, R. J. Steele, N. Barker *et al.*, 2010 Spindle orientation bias in gut epithelial stem cell compartments is lost in precancerous tissue. Cell Stem Cell 6**:** 175-181.

Ring, A., Y. M. Kim and M. Kahn, 2014 Wnt/catenin signaling in adult stem cell physiology and disease. Stem Cell Rev Rep 10**:** 512-525.

Robertson, S. M., and R. Lin, 2012 Our evolving view of Wnt signaling in C. elegans: If two's company and three's a crowd, is four really necessary? Worm 1**:** 82-89.

Rocheleau, C. E., W. D. Downs, R. Lin, C. Wittmann, Y. Bei *et al.*, 1997 Wnt signaling and an APC-related gene specify endoderm in early C. elegans embryos. Cell 90**:** 707-716.

Rocheleau, C. E., J. Yasuda, T. H. Shin, R. Lin, H. Sawa *et al.*, 1999 WRM-1 activates the LIT-1 protein kinase to transduce anterior/posterior polarity signals in C. elegans. Cell 97**:** 717-726.

Sawa, H., and H. C. Korswagen, 2013 Wnt signaling in C. elegans. WormBook**:** 1-30.

Sawa, H., L. Lobel and H. R. Horvitz, 1996 The Caenorhabditis elegans gene lin-17, which is required for certain asymmetric cell divisions, encodes a putative seven-transmembrane protein similar to the Drosophila frizzled protein. Genes Dev 10**:** 2189-2197.

Schlaitz, A. L., M. Srayko, A. Dammermann, S. Quintin, N. Wielsch *et al.*, 2007 The C. elegans RSA complex localizes protein phosphatase 2A to centrosomes and regulates mitotic spindle assembly. Cell 128**:** 115-127.

Sugioka, K., L. E. Fielmich, K. Mizumoto, B. Bowerman, S. van den Heuvel *et al.*, 2018 Tumor suppressor APC is an attenuator of spindle-pulling forces during C. elegans asymmetric cell division. Proc Natl Acad Sci U S A 115**:** E954-e963.

Sugioka, K., K. Mizumoto and H. Sawa, 2011 Wnt regulates spindle asymmetry to generate asymmetric nuclear β-catenin in C. elegans. Cell 146**:** 942-954.

Thompson, J. W., M. F. V. Michel and B. T. Phillips, 2022 Centrosomal enrichment and proteasomal degradation of SYS-1/β-catenin requires the microtubule motor dynein. Mol Biol Cell 33**:** ar42.

Timmons, L., 2006 Delivery methods for RNA interference in C. elegans. Methods Mol Biol 351**:** 119-125.

Umbhauer, M., A. Djiane, C. Goisset, A. Penzo-Méndez, J. F. Riou *et al.*, 2000 The C-terminal cytoplasmic Lys-thr-X-X-X-Trp motif in frizzled receptors mediates Wnt/beta-catenin signalling. Embo j 19**:** 4944-4954.

Vora, S., and B. T. Phillips, 2015 Centrosome-Associated Degradation Limits β-Catenin Inheritance by Daughter Cells after Asymmetric Division. Curr Biol 25**:** 1005-1016.

Vora, S. M., and B. T. Phillips, 2016 The benefits of local depletion: The centrosome as a scaffold for ubiquitin-proteasome-mediated degradation. Cell Cycle 15**:** 2124-2134.

Yamashita, Y. M., H. Yuan, J. Cheng and A. J. Hunt, 2010 Polarity in stem cell division: asymmetric stem cell division in tissue homeostasis. Cold Spring Harb Perspect Biol 2**:** a001313.

Yang, X. D., T. R. Karhadkar, J. Medina, S. M. Robertson and R. Lin, 2015 β-Catenin-related protein WRM-1 is a multifunctional regulatory subunit of the LIT-1 MAPK complex. Proc Natl Acad Sci U S A 112**:** E137-146.

Zacharias, A. L., and J. I. Murray, 2016 Combinatorial decoding of the invariant C. elegans embryonic lineage in space and time. Genesis 54**:** 182-197.

Zacharias, A. L., T. Walton, E. Preston and J. I. Murray, 2015 Quantitative Differences in Nuclear β-catenin and TCF Pattern Embryonic Cells in C. elegans. PLoS Genet 11**:** e1005585.

Figure 1

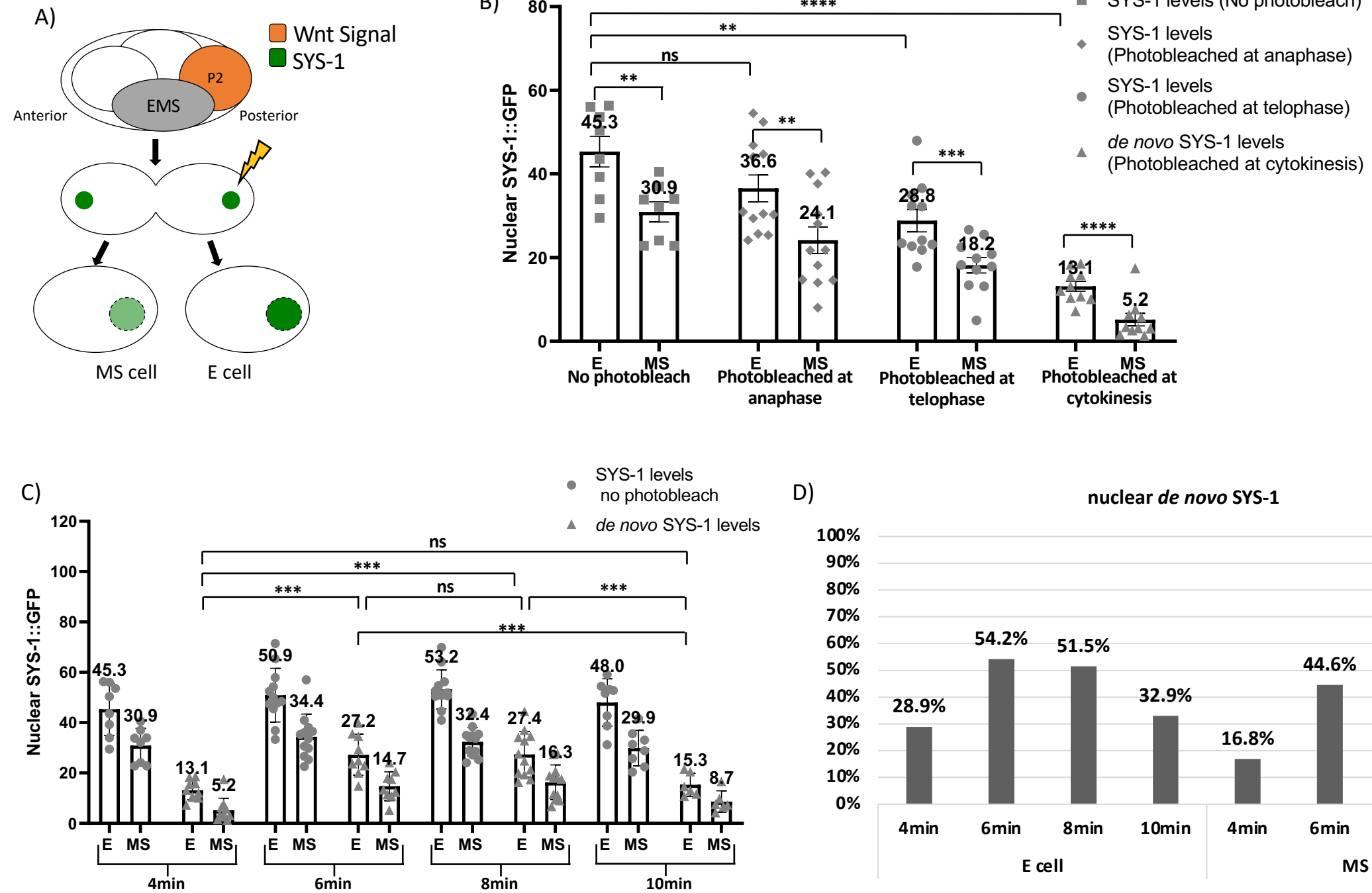
A)
Wnt Signal
SYS-1
P2
EMS
Anterior
Posterior
MS cell
E cell
B)
Nuclear SYS-1::GFP
SYS-1 levels (No photobleach)
SYS-1 levels (Photobleached at anaphase)
SYS-1 levels (Photobleached at telophase)
de novo SYS-1 levels (Photobleached at cytokinesis)
45.3
30.9
36.6
24.1
28.8
18.2
13.1
5.2
E MS
No photobleach
Photobleached at anaphase
Photobleached at telophase
Photobleached at cytokinesis
C)
SYS-1 levels no photobleach
de novo SYS-1 levels
Nuclear SYS-1::GFP
45.3
30.9
13.1
5.2
50.9
34.4
27.2
14.7
53.2
32.4
27.4
16.3
48.0
29.9
15.3
8.7
4min
6min
8min
10min
D)
nuclear de novo SYS-1
28.9%
54.2%
51.5%
32.9%
16.8%
44.6%
50.3%
28.5%
4min
6min
8min
10min
E cell
MS cell

Figure legends

Figure 1: Photobleaching reveals *de novo* and inherited SYS-1 pools in the E and MS cells and centrosomal SYS-1 dynamics over time.

A) Diagram of EMS cell Fluorescence After Photobleaching (FRAP) assay. The EMS cell is polarized by Wnt signaling from the P2 cell. The entire EMS mother cell is photobleached and SYS-1 nuclear levels are subsequently measured throughout the development of the E and the MS daughters. B) Quantification of nuclear SYS-1::GFP in E and MS cells following no photobleach (n=8), and photobleaching at anaphase (n=12), telophase (n=11), and cytokinesis (n=10). Fluorescence recordings were measured 4 min after mother cell division is complete. Mean +/- SEM. Student's two-tail t-test. C) Quantification of nuclear fluorescent SYS-1::GFP in the E and MS cells over time in non-bleached controls and EMS cell photobleached at cytokinesis. Mean +/- SEM. Student's two-tail t-test. D) Percentage of nuclear SYS-1 in the daughter cells during a 2 min interval timecourse elucidates *de novo* translated SYS-1 dynamics in the E and MS daughter cells over time. N= denoted by grey figures in graph. * $p \leq 0.05$, ** $p \leq 0.01$, *** $p \leq 0.001$, **** $p \leq 0.0001$

Figure 2

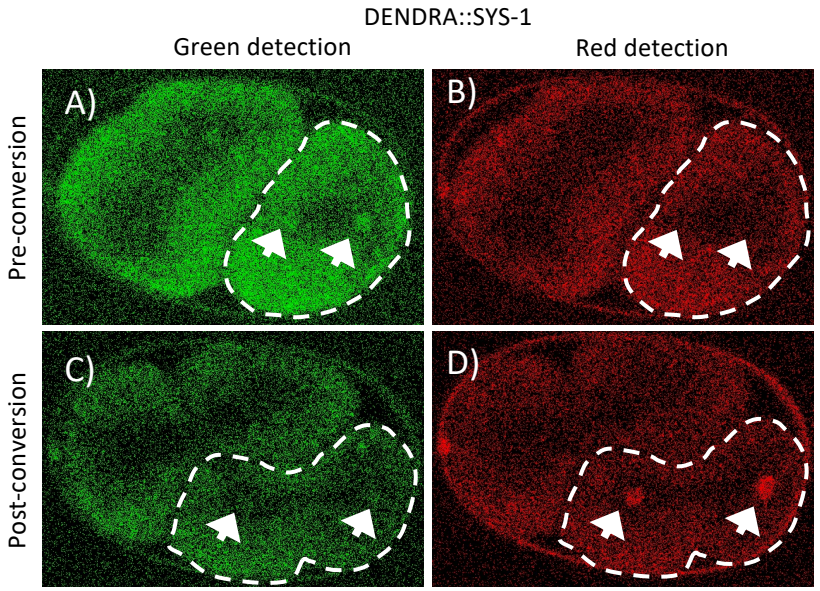
DENDRA::SYS-1
Green detection
Red detection
Pre-conversion
Post-conversion
A)
B)
C)
D)

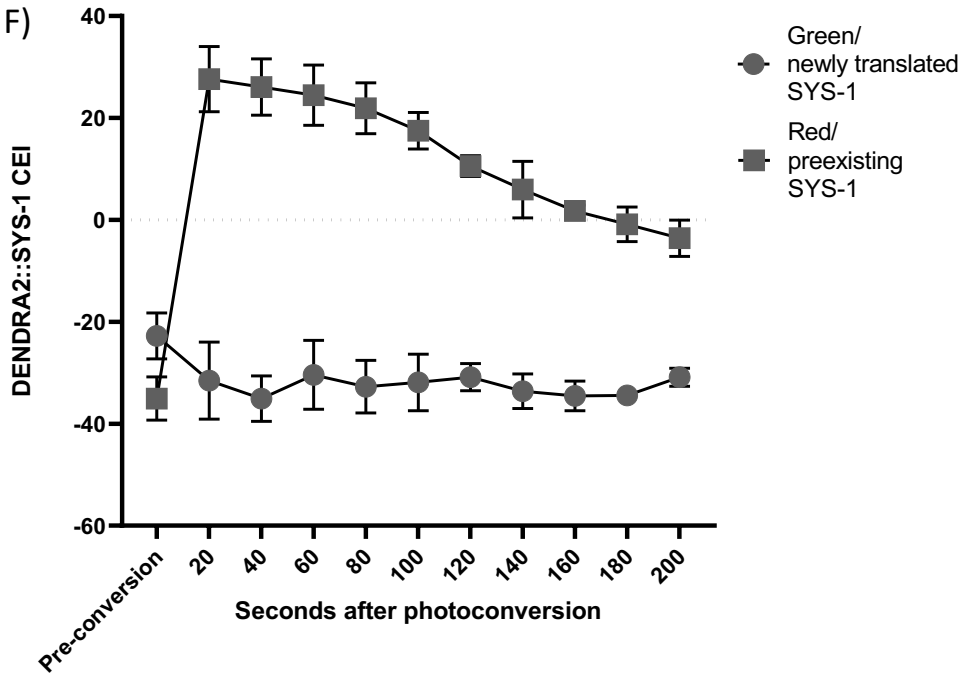
F)
DENDRA2::SYS-1 CEI
40
20
0
-20
-40
-60
Pre-conversion
20
40
60
80
100
120
140
160
180
200
Seconds after photoconversion
Green/
newly translated
SYS-1
Red/
preexisting
SYS-1

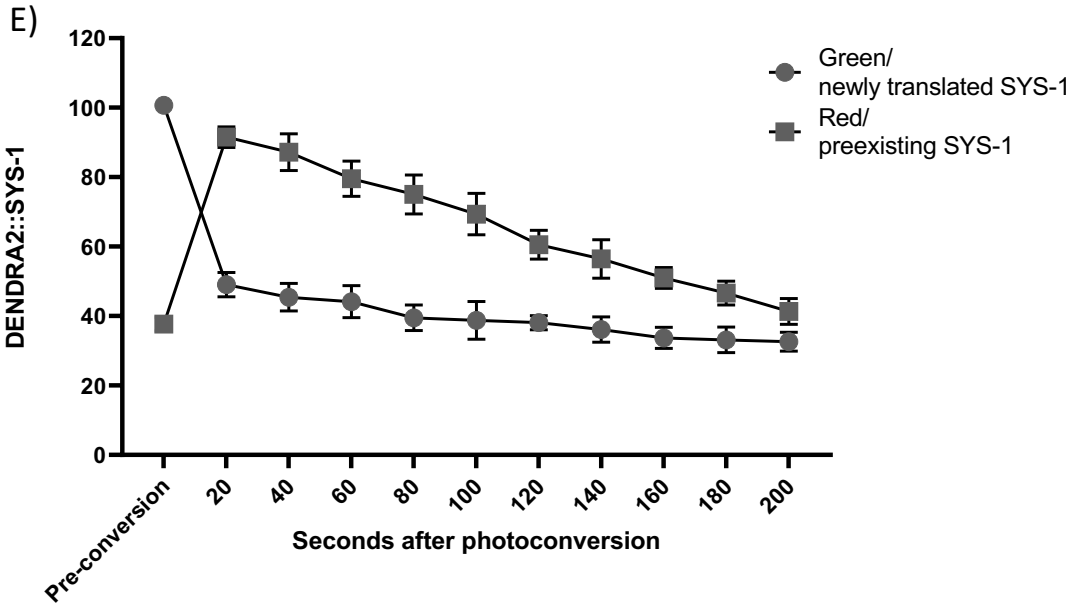
E)
DENDRA2::SYS-1
120
100
80
60
40
20
0
Pre-conversion
20
40
60
80
100
120
140
160
180
200
Seconds after photoconversion
Green/
newly translated SYS-1
Red/
preexisting SYS-1

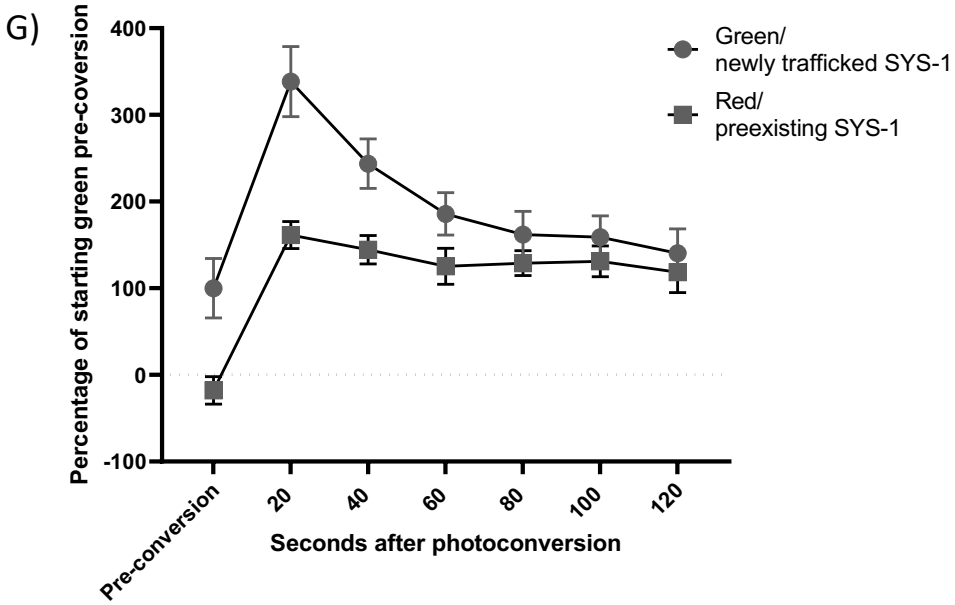
G)
Percentage of starting green pre-coversion
400
300
200
100
0
-100
Pre-conversion
20
40
60
80
100
120
Seconds after photoconversion
Green/
newly trafficked SYS-1
Red/
preexisting SYS-1

Figure 2: <u>Photoconversion of DENDRA2::SYS-1 reveals turnover at the centrosome during mitosis.</u>
A) Pre-conversion image shows centrosomal localization of DENDRA2::SYS-1 in the green channel.
B) Centrosomal DENDRA2::SYS-1 is undetectable in the red channel prior to photoconversion by 405nm blue laser exposure. C) After photoconversion newly translated DENDRA2::SYS-1 is trafficked to the centrosome, and D) shows photoconverted DENDRA2::SYS-1 at the centrosome. E) Quantification of average centrosomal DENDRA2::SYS-1 in both channels over time. Mean +/- SEM. N=3. F) Centrosomal enrichment index (CEI) of the time course shown in (E). Mean +/- SEM. N=3. CEI was calculated in FIJI by subtracting the mean pixel intensity of a cytoplasmic ROI encompassing the posterior half of the cell with the dotted white line (A–D), from a circular centrosome ROI. G) Percentage of starting green fluorescence. Each data point was the average quantification of green or red centrosomal DENDRA2::SYS-1, respectively, divided by the pre-conversion green centrosomal DENDRA2::SYS-1 levels. Mean with SEM. N=7.

Figure 3

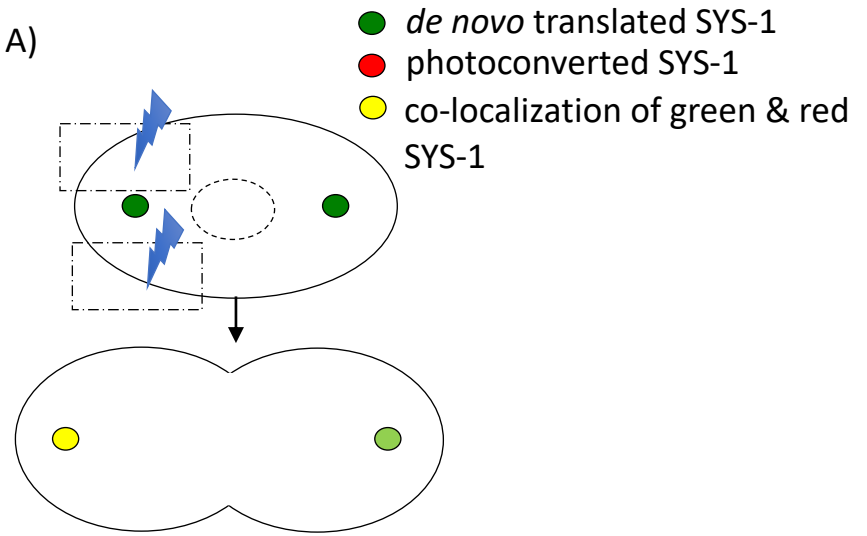
A)
de novo translated SYS-1
photoconverted SYS-1
co-localization of green & red SYS-1

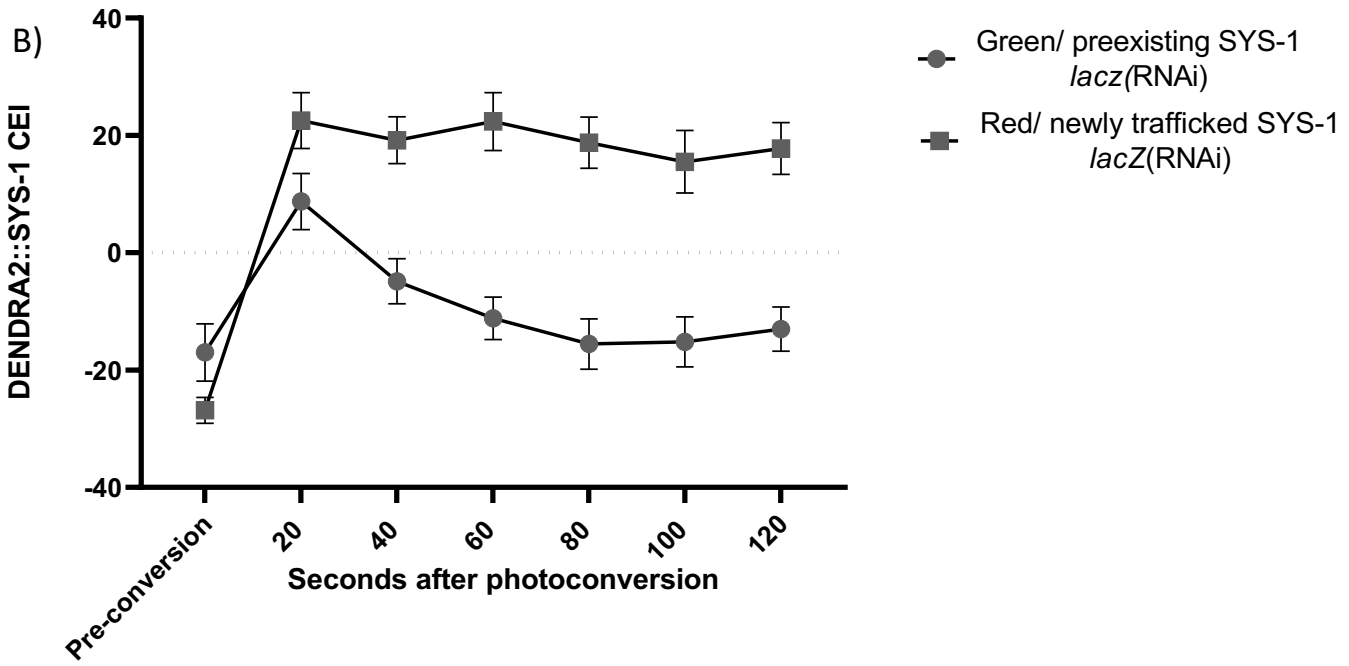
B)
DENDRA2::SYS-1 CEI
40
20
0
-20
-40
Pre-conversion
20
40
60
80
100
120
Seconds after photoconversion
Green/ preexisting SYS-1 *lacz*(RNAi)
Red/ newly trafficked SYS-1 *lacZ*(RNAi)

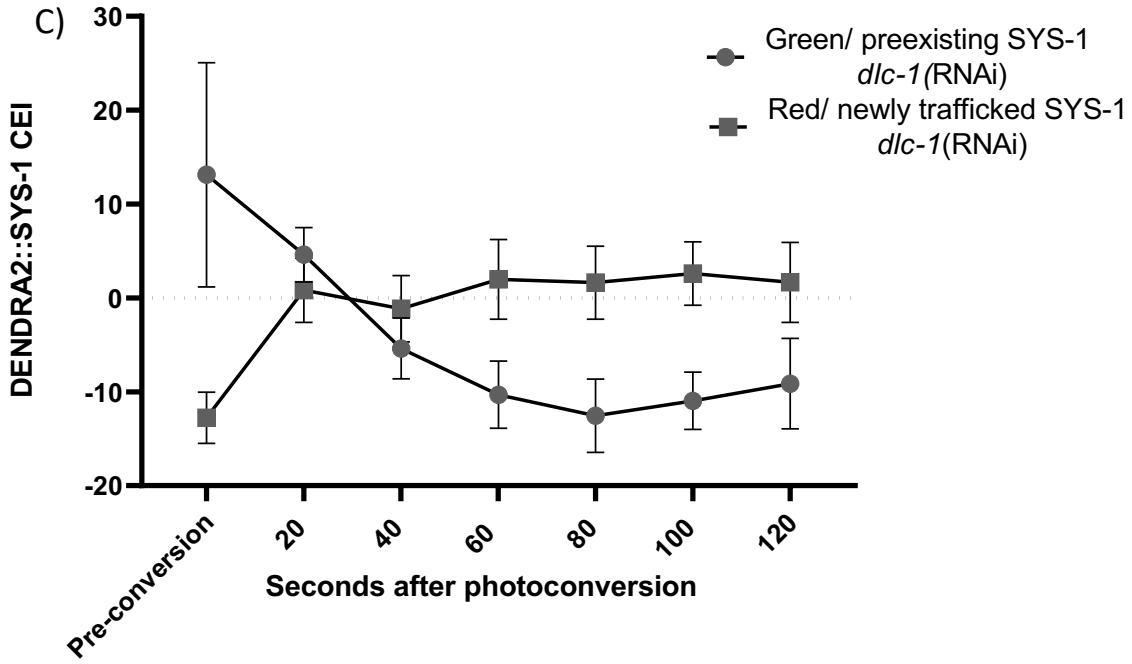
C)
DENDRA2::SYS-1 CEI
30
20
10
0
-10
-20
Pre-conversion
20
40
60
80
100
120
Seconds after photoconversion
Green/ preexisting SYS-1 *dlc-1*(RNAi)
Red/ newly trafficked SYS-1 *dlc-1*(RNAi)

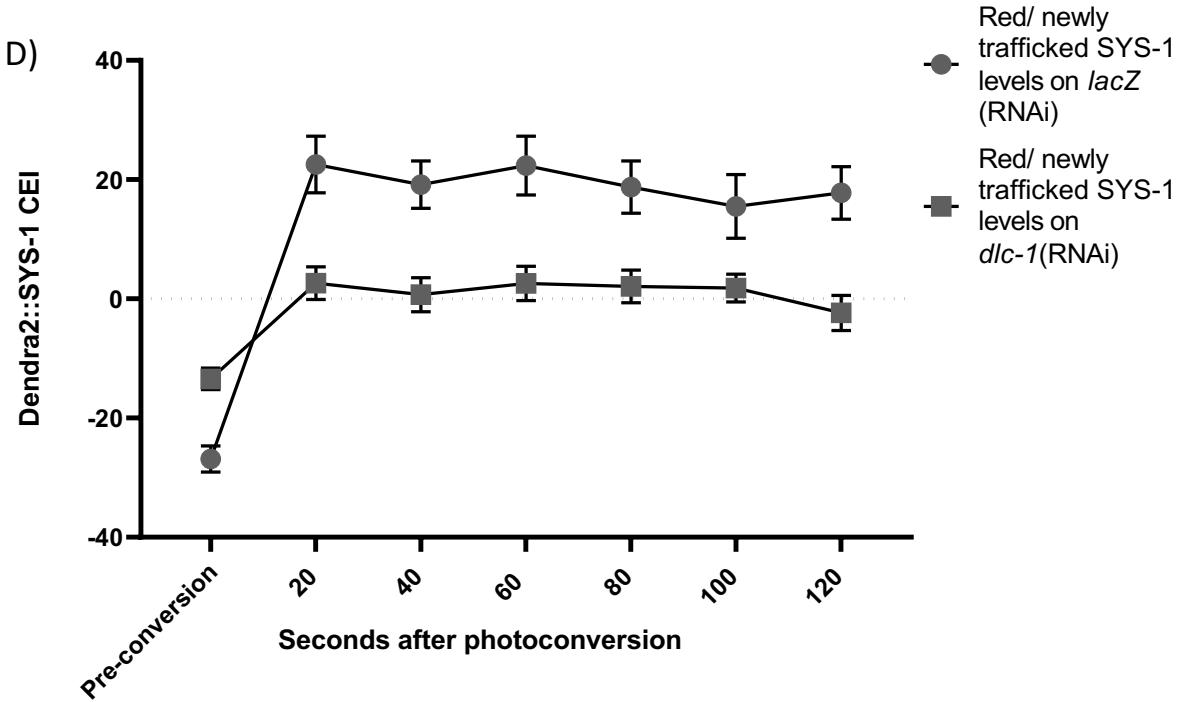
D)
Dendra2::SYS-1 CEI
40
20
0
-20
-40
Pre-conversion
20
40
60
80
100
120
Seconds after photoconversion
Red/ newly trafficked SYS-1 levels on *lacZ* (RNAi)
Red/ newly trafficked SYS-1 levels on *dlc-1*(RNAi)

Figure 3: <u>Photoconversion of the cytoplasm of the P1 cell unveils dynamics of dynein trafficking of DENDRA2::SYS-1 during mitosis.</u>

A) Diagram of photoconversion of the P1 cell. Dotted square represents the photoconverted area of the cytoplasm at metaphase. B) Quantification of green and red DENDRA2::SYS-1 centrosomal enrichment index (CEI) pre- and post-photoconversion of the cytoplasm, measured over a 2 min timecourse in 20 s intervals after photoconversion on control *lacZ*(RNAi). Mean +/-SEM. N=12. CEI was calculated in FIJI by subtracting the mean pixel intensity of a cytoplasmic ROI encompassing the posterior half of the cell with the dotted white line (Fig. 2A-D), from a circular centrosome ROI. C) Quantification of green and red DENDRA2::SYS-1 CEI after photoconversion of cytoplasm on *dlc-1*(RNAi). Mean +/-SEM. N=15. D) Timecourse depicting red, photoconverted DENDRA2::SYS-1 CEI on *lacZ*(RNAi) and *dlc-1*(RNAi). Mean +/-SEM. N= 12 and 15, respectively.

Figure 4

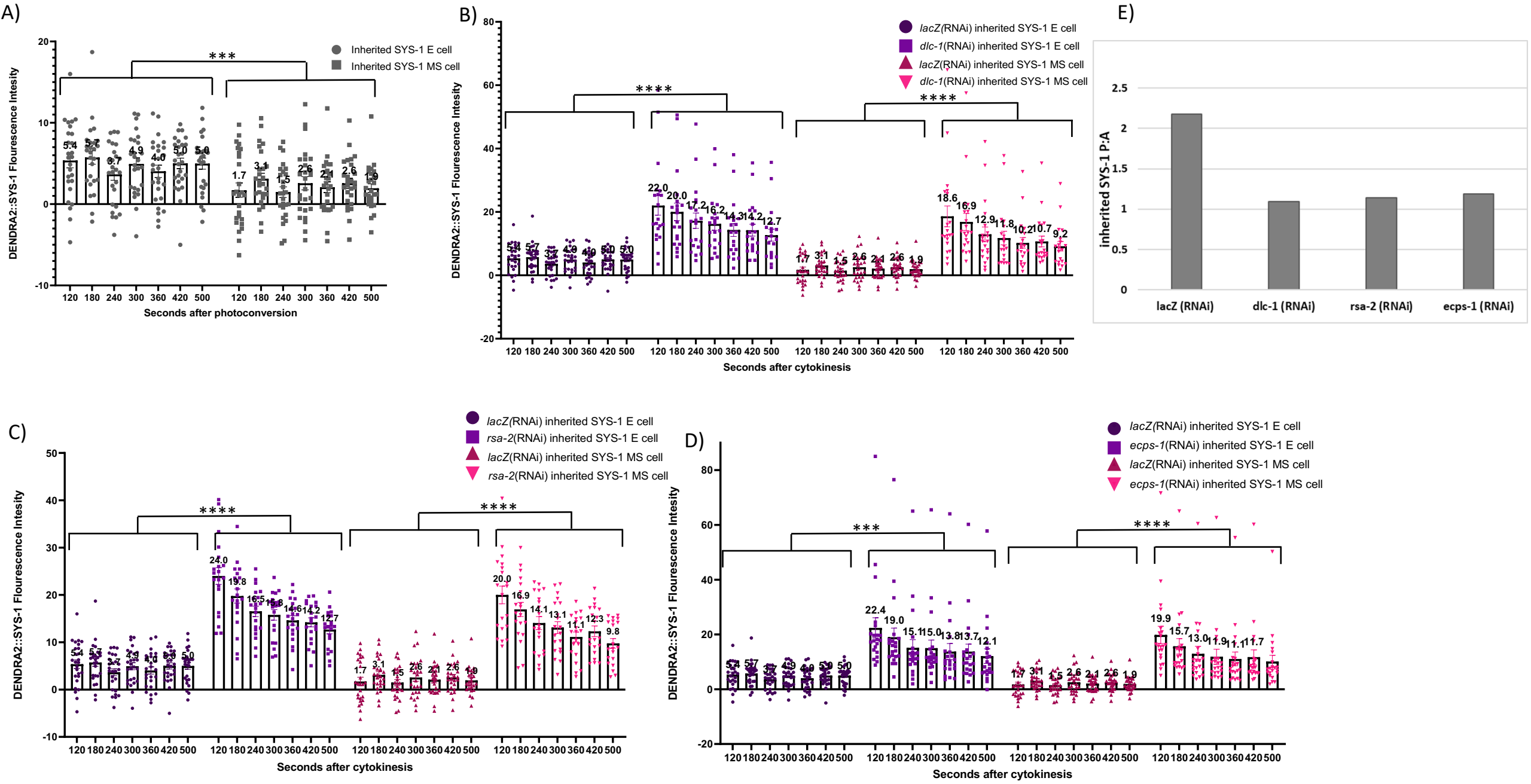
A)
Inherited SYS-1 E cell
Inherited SYS-1 MS cell
***
DENDRA2::SYS-1 Flourescence Intesity
Seconds after photoconversion
B)
lacZ(RNAi) inherited SYS-1 E cell
dlc-1(RNAi) inherited SYS-1 E cell
lacZ(RNAi) inherited SYS-1 MS cell
dlc-1(RNAi) inherited SYS-1 MS cell
****
****
DENDRA2::SYS-1 Flourescence Intesity
Seconds after cytokinesis
E)
inherited SYS-1 P:A
lacZ (RNAi)
dlc-1 (RNAi)
rsa-2 (RNAi)
ecps-1 (RNAi)
C)
lacZ(RNAi) inherited SYS-1 E cell
rsa-2(RNAi) inherited SYS-1 E cell
lacZ(RNAi) inherited SYS-1 MS cell
rsa-2(RNAi) inherited SYS-1 MS cell
****
****
DENDRA2::SYS-1 Flourescence Intesity
Seconds after cytokinesis
D)
lacZ(RNAi) inherited SYS-1 E cell
ecps-1(RNAi) inherited SYS-1 E cell
lacZ(RNAi) inherited SYS-1 MS cell
ecps-1(RNAi) inherited SYS-1 MS cell
***
****
DENDRA2::SYS-1 Flourescence Intesity
Seconds after cytokinesis

Figure 4: <u>E and MS inheritance of mother cell SYS-1 is limited by EMS centrosomal processing.</u>
A) Quantification of inherited, red DENDRA2::SYS-1 nuclear levels of the E and MS cells at different timepoints starting 2 m after cytokinesis of the EMS mother cell in 60 second increments on the control *lacZ*(RNAi). Mean +/-SEM. 2way ANOVA followed by Tukey Mixed effects analysis in Multiple Comparisons test. N=12. B) Quantification of inherited, red DENDRA2::SYS-1 nuclear levels of the E and MS cells timecourse on control vs. *dlc-1*(RNAi) (N=26 and N=20, respectively). Mean +/-SEM. 2way ANOVA followed by Sidak Mixed effects analysis in Multiple Comparisons test. C) Quantification of inherited, red DENDRA2::SYS-1 nuclear levels of the E and MS daughter cells timecourse on control vs. *rsa-2*(RNAi) (N=26 and N=20, respectively). Mean +/-SEM. 2way ANOVA followed by Sidak Mixed effects analysis in Multiple Comparisons test. D) Quantification of inherited, red DENDRA2::SYS-1 nuclear levels of the E and MS daughter cells timecourse on control vs. *ecps-1*(RNAi) (n=26 and n=20, respectively). Mean +/-SEM. 2way ANOVA followed by Sidak Mixed effects analysis in Multiple Comparisons test. E) Quantification of fold change in asymmetry between the E and MS cells in *lacZ, dlc-1, rsa-2 and ecps-1,* (RNAi). DENDRA2::SYS-1 fluorescent intensity was calculated by subtracting N2 fluorescence at all different timepoints. * represent the P-value when comparing the averaged value of all time points of *lacZ(*RNAi) to experimental condition. Table S1. P-values when comparing each time point. * $p \leq 0.05$, ** $p \leq 0.01$, *** $p \leq 0.001$, **** $p \leq 0.0001$

Figure 5

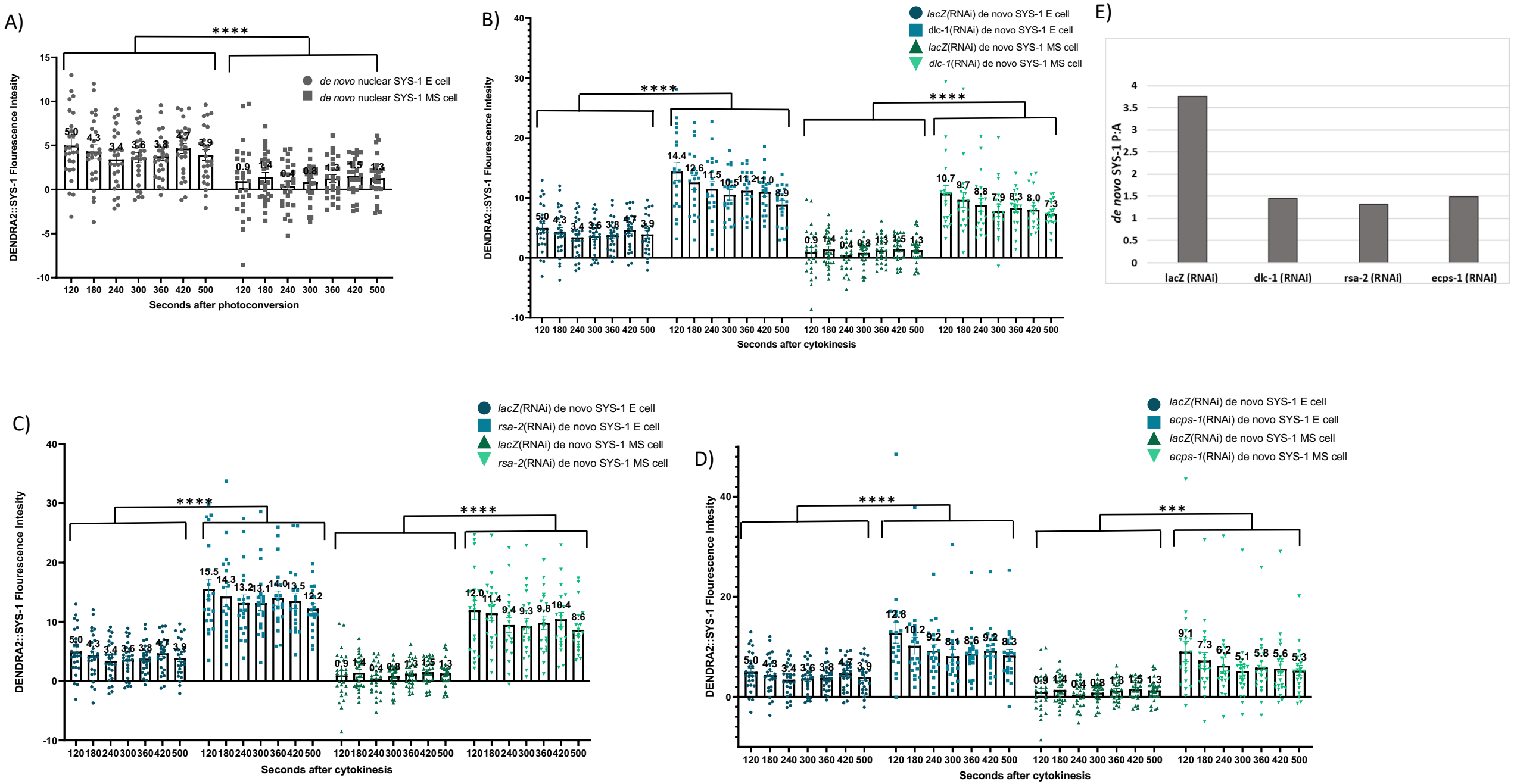
A)
****
de novo nuclear SYS-1 E cell
de novo nuclear SYS-1 MS cell
DENDRA2::SYS-1 Flourescence Intesity
Seconds after photoconversion
B)
lacZ(RNAi) de novo SYS-1 E cell
dlc-1(RNAi) de novo SYS-1 E cell
lacZ(RNAi) de novo SYS-1 MS cell
dlc-1(RNAi) de novo SYS-1 MS cell
DENDRA2::SYS-1 Flourescence Intesity
Seconds after cytokinesis
E)
de novo SYS-1 P:A
lacZ (RNAi)
dlc-1 (RNAi)
rsa-2 (RNAi)
ecps-1 (RNAi)
C)
lacZ(RNAi) de novo SYS-1 E cell
rsa-2(RNAi) de novo SYS-1 E cell
lacZ(RNAi) de novo SYS-1 MS cell
rsa-2(RNAi) de novo SYS-1 MS cell
DENDRA2::SYS-1 Flourescence Intesity
Seconds after cytokinesis
D)
lacZ(RNAi) de novo SYS-1 E cell
ecps-1(RNAi) de novo SYS-1 E cell
lacZ(RNAi) de novo SYS-1 MS cell
ecps-1(RNAi) de novo SYS-1 MS cell
***
DENDRA2::SYS-1 Flourescence Intesity
Seconds after cytokinesis

Figure 5: <u>Loss of centrosomal SYS-1 results in increased levels of nuclear *de novo* SYS-1 in EMS daughter cells</u>. A) Quantification of green/*de novo* SYS-1 nuclear levels in the E and MS cells after photoconversion of the EMS cell at cytokinesis; the timecourse depicts SYS-1 nuclear levels at different timepoints starting 2 minutes after cytokinesis of the EMS cell in 60 second increments on the control *lacZ*(RNAi) (n=26). Mean+/- SEM. 2way ANOVA followed by Sidak Mixed effects analysis in Multiple Comparisons test. B) Quantification of *de novo* SYS-1 nuclear levels of the E and MS cells timecourse on *lacZ(RNAi)* and *dlc-1*(RNAi) (n=26 and n=20, respectively). Mean +/-SEM. 2way ANOVA followed by Sidak Mixed effects analysis in Multiple Comparisons test. C) Quantification of *de novo* SYS-1 nuclear levels of the E and MS cells timecourse on *lacZ(RNAi)* and *rsa-2*(RNAi) (n=26 and n=20, respectively). Mean +/- SEM. 2way ANOVA followed by Sidak Mixed effects analysis in Multiple Comparisons test. D) Quantification of *de novo* SYS-1 nuclear levels of the E and MS cells timecourse on *lacZ(RNAi)* and *ecps-1*(RNAi) (n=26 and n=20, respectively). Mean+/- SEM. 2way ANOVA followed by Sidak Mixed effects analysis in Multiple Comparisons test. E) Quantification of fold change in asymmetry between the E and MS daughter cell in *lacZ, dlc-1, rsa-2 and ecps-1* (RNAi). DENDRA2::SYS-1 fluorescent intensity was calculated by subtracting N2 fluorescence at all different timepoints. * represent the P-value when comparing all time points and the average of control to experimental condition. Table S1. P-values when comparing each time point. * $p \leq 0.05$, ** $p \leq 0.01$, *** $p \leq 0.001$, **** $p \leq 0.0001$

Figure 6

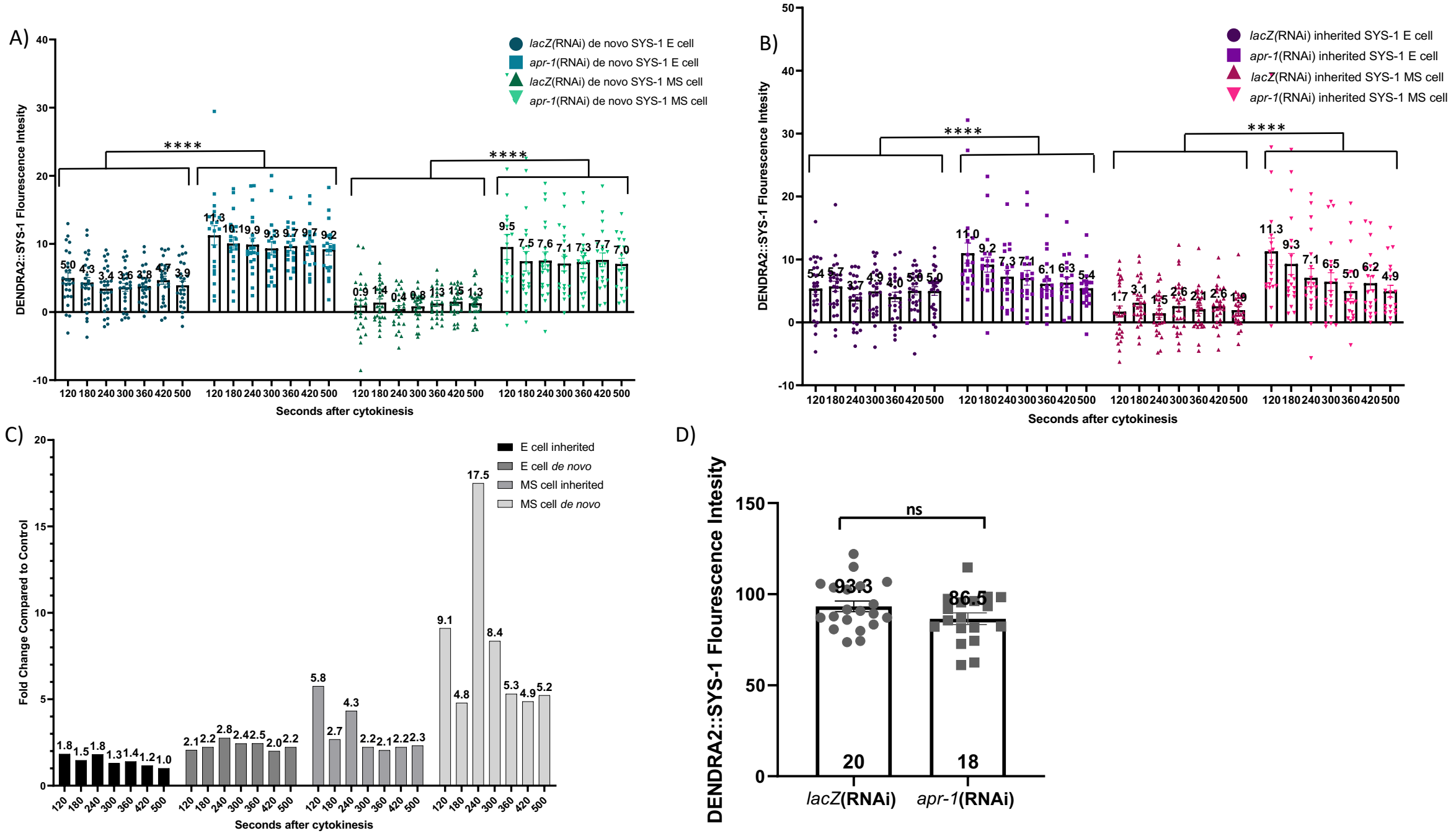
A)
lacZ(RNAi) de novo SYS-1 E cell
apr-1(RNAi) de novo SYS-1 E cell
lacZ(RNAi) de novo SYS-1 MS cell
apr-1(RNAi) de novo SYS-1 MS cell
DENDRA2::SYS-1 Flourescence Intesity
Seconds after cytokinesis
****
****
B)
lacZ(RNAi) inherited SYS-1 E cell
apr-1(RNAi) inherited SYS-1 E cell
lacZ(RNAi) inherited SYS-1 MS cell
apr-1(RNAi) inherited SYS-1 MS cell
DENDRA2::SYS-1 Flourescence Intesity
Seconds after cytokinesis
****
****
C)
E cell inherited
E cell de novo
MS cell inherited
MS cell de novo
Fold Change Compared to Control
Seconds after cytokinesis
D)
ns
93.3
86.5
20
18
DENDRA2::SYS-1 Flourescence Intesity
lacZ(RNAi)
apr-1(RNAi)

Figure 6: <u>Partial loss of the negative regulator of the Wnt signaling pathway, APR-1, affects both pools of nuclear SYS-1 in the E and MS cells</u>. A) Quantification of *de novo* SYS-1 nuclear levels in the E and MS cells after photoconversion at cytokinesis over 7-minute timecourse on *lacZ(RNAi) and apr-1* (RNAi) (n=26 and n=20, respectively). Mean +/-SEM. 2way ANOVA followed by Sidak Mixed effects analysis in Multiple Comparisons test. B) Quantification of inherited SYS-1 nuclear levels in the E and MS cells after photoconversion at cytokinesis over 7-minute timecourse on *lacZ(RNAi) and apr-1* (RNAi). Mean +/-SEM. 2way ANOVA followed by Sidak Mixed effects analysis in Multiple Comparisons test. C) Graph representation of the fold change in *de* novo and inherited nuclear SYS-1 of APR-1 compared to the control in the E and MS cells. D) Quantification of centrosomal DENDRA2::SYS-1 levels in the EMS cell on *lacZ(RNAi)* and *apr-1* (RNAi) (n=20 and n=18, respectively). Mean +/-SEM. Unpaired two-tail t-test. * represent the P-value when comparing all time points and the average of control to experimental condition. Table S1. P-values when comparing each time point. DENDRA2::SYS-1 fluorescent intensity was calculated by subtracting N2 fluorescence at all different timepoints. * $p \leq 0.05$, ** $p \leq 0.01$, *** $p \leq 0.001$, **** $p \leq 0.0001$

Figure 7

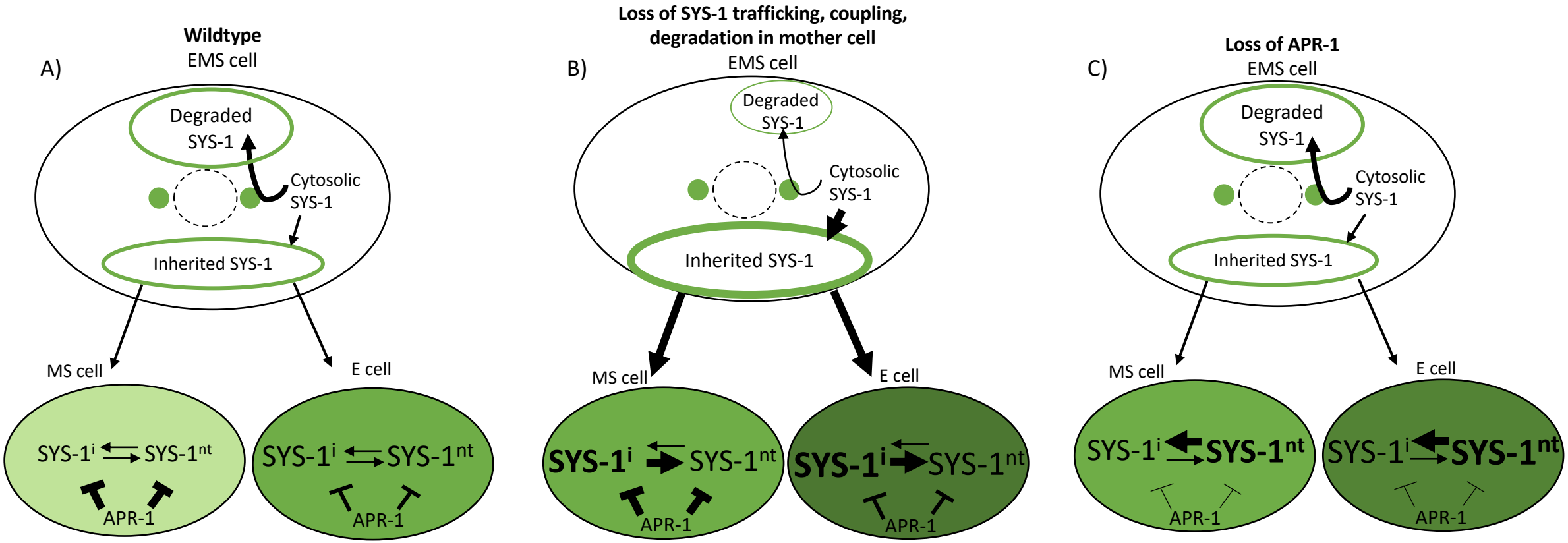
A)
Wildtype
EMS cell
Degraded SYS-1
Cytosolic SYS-1
Inherited SYS-1
MS cell
E cell
SYS-1i
SYS-1nt
APR-1
B)
Loss of SYS-1 trafficking, coupling, degradation in mother cell
EMS cell
Degraded SYS-1
Cytosolic SYS-1
Inherited SYS-1
MS cell
E cell
SYS-1i
SYS-1nt
APR-1
C)
Loss of APR-1
EMS cell
Degraded SYS-1
Cytosolic SYS-1
Inherited SYS-1
MS cell
E cell
SYS-1i
SYS-1nt
APR-1

Figure 7: <u>Model for SYS-1 regulation during ACD</u>. A) In wildtype, in the EMS cell, cytosolic SYS (green) is trafficked to the centrosome via dynein where it gets degraded by the centrosomal proteosome. The remaining cytosolic SYS-1 is inherited into the E and MS cells where it is regulated by APR-1. The inherited and the *de novo* pools in both daughter cells are freely exchanged, stably maintaining the pools through the cell cycle. In the MS cell, APR-1 lowers SYS-1 levels such that it is asymmetric compared to the E cell, which has reduced APR-1 activity. B) Loss of SYS-1 mother cell regulation, including loss of SYS-1 centrosomal trafficking, coupling or degradation, decreases degradation of the cytosolic SYS-1 at the centrosome, leading to increased SYS-1 inheritance into both daughter cells (bold arrows). In the E and MS cell the increased inherited SYS-1 leads to an increased *de novo* pool. APR-1 is unable to bring SYS-1 levels down to basal levels, which leads to higher levels of both SYS-1 pools and a loss of SYS-1 asymmetry between the E and MS cell. C) Loss of APR-1 has no effect in the EMS cell, however, APR-1 depletion leads to an increased *de novo* SYS-1 pool, which in turn, affects the inherited pool, since the cell is unable to bring SYS-1 back to basal levels in both daughters. Higher levels of both pools in the E and MS nuclei lead to a loss of SYS-1 asymmetry. The weight of the arrows and lines represent the relative changed effect, font size represents size of the relevant SYS-1 pool. SYS-1^{i}, inherited SYS-1; SYS-1^{nt}, newly translated SYS-1.